AN INVESTIGATION INTO HIGH SPEED CRACK PROPAGATION AND BRANCHING USING A HYBRID EXPERIMENTAL - FEM APPROACH

By

KAVATURU MAHESH

ME

1995

M

MAH

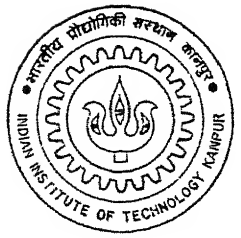

DEPARTMENT OF MECHANICAL ENGINEERING

AN INVESTIGATION INTO HIGH SPEED CRACK PROPAGATION AND BRANCHING USING A HYBRID EXPERIMENTAL - FEM APPROACH

A Thesis Submitted
in Partial Fulfilment of the Requirements
for the Degree of

MASTER OF TECHNOLOGY

By
KAVATURU MAHESH

to the

DEPARTMENT OF MECHANICAL ENGINEERING

INDIAN INSTITUTE OF TECHNOLOGY, KANPUR

June, 1995

CERTIFICATE

It is certified that the work contained in the thesis entitled **AN INVESTIGATION INTO HIGH SPEED CRACK PROPAGATION AND BRANCHING USING A HYBRID EXPERIMENTAL - FEM APPROACH**, by **Kavaturu Mahesh**, has been carried out under my supervision and has not been submitted elsewhere for the award of a degree.

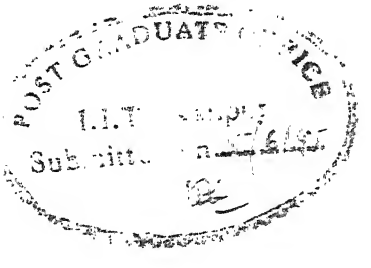

N.N. Kishore 5/6/95
N.N.Kishore
Professor
Mechanical Engg. Dept
I.I.T Kanpur

ACKNOWLEDGEMENTS

I take this opportunity to express my sincere gratitude to **Prof. N.N. Kishore** for his supervision and perspicacious guidance. I am highly indebted to him for his help, support and friendly disposition.

A special note of gratitude is extended to Dr. Arun Shukla for his invaluable suggestions in carrying out the experiments. I am grateful to Dr. B.D Agarwal for extending the facilities of the dynamic photo-mechanics laboratory. A personal note of appreciation goes to Dr. Prashant Kumar for the fruitful discussions I had with him throughout my M.Tech.

I am highly thankful to S.K.Verma, K.K.Bajpai and J. Yadav for their constant help and encouragement. I express my thanks to S.K.Trivedi for his help in fabricating the loading frame and the specimens for the experiments. S.Ravi and D.Datta deserve a special mention for their encouragement throughout this endeavor.

I am very much thankful to K.S.Rao and S.Ravi for their help in the preparation of the thesis. A special note of thanks go to my friends Murthy, TAN, B.V.N.Rao, Subbarao, Vishwas Kher, Subrahmanyam, Anil, B.C.Rao for their support, help, encouragement and affection.

Finally, I wish to acknowledge my parents and siblings for their affection and help in making my dreams come true.

Mahesh

Dedicated to my Parents
Siblings
&
Alter ego

CONTENTS

1. INTRODUCTION 1
1.1 STATE OF THE ART SURVEY 3
1.2 OBJECTIVE OF THE PRESENT WORK 6
1.3 LAYOUT OF THE THESIS 7

2. FINITE ELEMENT MODELLING OF CRACK PROPAGATION AND BRANCHING 8
2.1 THEORY OF LINEAR ELASTO-DYNAMICS 8
2.2 BASICS OF DYNAMIC FRACTURE 13
2.3 MODELLING OF CRACK PROPAGATION AND BRANCHING 13
2.3.1 Stationary Mesh Procedure 15
2.4 SPATIAL AND TEMPORAL DESCRETIZATION 17
2.5 NEWMARK'S METHOD 19
2.6 BOUNDARY AND INITIAL CONDITIONS 19
2.7 ERROR AND STABILITY CONSIDERATIONS 20
2.8 CALCULATION OF $\hat{J}_1$-INTEGRAL 21
2.9 COMPUTER IMPLEMENTATION 22

3. EXPERIMENTAL TECHNIQUE 23
3.1 EXPERIMENTAL DETAILS 23
3.2 MEASUREMENT OF CRACK PROPAGATION SPEED 25
3.3 EXPERIMENTAL PROCEDURE 25

4. RESULTS AND DISCUSSION 30
4.1 EXPERIMENTAL OBSERVATIONS 30
4.2 NUMERICAL MODELLING 32

4.3 DISCUSSIONS 38

5. CONCLUSIONS AND SCOPE FOR FURTHER WORK 46

5.1 CONCLUSIONS 46

5.2 SCOPE FOR FUTURE WORK 46

REFERENCES 48

APPENDIX-A 52

LIST OF TABLES

Table 4.1 Experimental observations and results 45
Table 4.2 Variation of J_{1b} with velocity 45

LIST OF FIGURES

Fig. 2.1 Generalized body 9
Fig. 2.2 Computational modelling of crack propagation and branching 14
Fig. 2.3 Holding back forces on the double node 16
Fig. 2.4 Gradual node release techniques 18
Fig. 2.5 Contours for path-independent integrals 21
Fig. 3.1 Loading Frame 24
Fig. 3.2 Electronic circuit for propagation gauges 26
Fig. 3.3 Schematic diagram of the specimen 27
Fig. 3.4 Typical record of the oscilloscope 28
Fig. 4.1a Oscilloscope record for Experiment # 1 33
Fig. 4.1b Crack tip location as a function of time for Expt.# 1 33
Fig. 4.2a Oscilloscope record for Expt. # 2 34
Fig. 4.2b Crack tip location as a function of time for Expt.# 2 34
Fig. 4.3a Oscilloscope record for Expt. # 3 35
Fig. 4.3b Crack tip location as a function of time for Expt.# 3 35
Fig. 4.4a Oscilloscope record for Expt. # 4 36
Fig. 4.4b Crack tip location as a function of time for Expt.# 4 36
Fig. 4.5a Photograph of the fractured specimen in Expt.# 3 37
Fig. 4.5b Photograph of the fractured specimen in Expt. # 4 37
Fig. 4.6 $\hat{J}_1$ and crack-tip location as a function of time for Expt. # 1 41
Fig. 4.7 $\hat{J}_1$ and crack-tip location as a function of time for Expt. # 2 41
Fig. 4.8 $\hat{J}_1$ and crack-tip location as a function of time for Expt. # 3 42
Fig. 4.9 $\hat{J}_1$ and crack-tip location as a function of time for Expt. # 4 43
Fig. 4.10 Photograph of the fractured surface (50x) 44

CHAPTER 1

INTRODUCTION

An understanding of the mechanics of dynamic fracture is necessary for developing sound design methodologies aimed at assuring the integrity of structures under dynamic loading conditions. The subject of the mechanics of dynamic fracture - that is fracture wherein the effect of inertia forces is important in determining crack propagation phenomena - can be broadly described as that of mechanics of solids, containing stationary or propagating cracks, wherein the effects of material inertia and stress wave interactions play significant roles.

Quasi-static crack growth has received a great deal of attention since the inception of Griffith and the mechanics of quasi-static fracture of linear-elastic, plastic and linear visco-elastic materials are quite well understood. On the other hand, dynamic fracture has received relatively little attention mainly due to the complex nature of the problem. There is however, substantial interest in the dynamic fracture problem due to its importance in many engineering applications. The problem is encountered in impact damage to fan blades, automobile and aircraft wind shields, nuclear reactors, pipe lines, rocket motors etc.. In mining and oil recovery operations, one wishes to increase the rock porosity through explosively induced fracture. In these problems, an understanding of the physics of crack branching is important. Also there is considerable interest in the problem of crack arrest of a fast running crack, especially with respect to large structures like pipe lines, ships and nuclear reactors. Crack branching is most often observed in practice, especially in the case of brittle cleavage cracks propagating at high speed. The branching of cracks in a shattering window pane are well known. Exploding pressure vessels may torn apart in many pieces as a result of crack branching.

One logical way of classifying dynamic fracture problems is as follows:

1. Solids, containing stationary cracks, subjected to dynamic loading

2. Solids, containing dynamically propagating cracks, under quasi-static loading; and
3. Solids, containing, dynamically propagating cracks under dynamic loads

Problems under categories (1) and (2) have recently received wide attention of late, than those under categories (3). To study, experimentally, the processes of dynamic fracture, several test procedures and several types of specimens geometries have been devised. These include charpy-test, Dynamic Tear (DT) test etc. which fall into category (1) mentioned above and test on the Double Cantilever Beam (DCB) and Compact Tension (CT) specimen, etc., which fall into problem category (2) above. These specimen tests, especially that on the DCB, aim to assess the crack arrest capabilities of structural materials.

A knowledge of time-dependent asymptotic stress and displacement fields near the crack tip, and their *strength* as quantified, for instance, by the stress intensity factors in linear elasto-dynamics, is essential in understanding the process and nature of fast fracture in solids. A most direct approach to a laboratory evaluation of dynamic fracture toughness and crack arrest toughness, makes use of the measurements of the instantaneous dynamic stress field close to the propagating crack-tip. While notable successes have been achieved in this area, such direct measurements using optical techniques are generally difficult, in non-transparent structural steel specimens of practical interest. To overcome these difficulties, hybrid experimental-numerical methods are often preferred [Kobayishi, 1983, Atluri and Nishioka, 1984]. Thus the advancement of dynamic fracture mechanics relies heavily on simultaneous advances in computational methods for a complete analysis of dynamic crack propagation problems.

A number of analytical solutions to problems of dynamic fracture, which shed important light on the basic phenomena involved, have been obtained in the past. These solutions, are limited to cases of simple loadings and of unbounded plane bodies. However the interactions of stress wave emanating from the crack-tip and/or those reflected from boundaries make the closed-form solutions of the dynamic fracture in finite bodies

intractable. Thus, it is often becomes mandatory to use computational methods to analyze problems of crack propagation in finite solids.

The advent of high speed computers has revolutionized the numerical modelling of linear and non-linear elasto-dynamics. Numerical models play an important role to understand the dynamic crack propagation and the inverse problems. The application of the finite element method (FEM) as a numerical tool to determine crack-tip stress fields and thereby the stress intensity factors has been in rapid progress. The method has great versatility, and it allows the analysis of complicated engineering geometries, materials and loadings.

1.1 STATE OF THE ART SURVEY

Considerable analytical as well as experimental effort has gone into investigating the problems of crack initiation, arrest, propagation and branching, but there remain a number of unanswered and partially answered questions. In this section a detailed literature survey of crack initiation, arrest, propagation and branching is presented.

Following Griffith [1921, 1924], the criterion for crack initiation can be stated quite simply : the energy required to create new surfaces must be equal to that released by the solid in deforming to the new configuration. Of course, energy required to create new surfaces, or equivalently the critical stress intensity factor, has to be determined for each material through experiments. Under dynamic loading conditions, the energy criterion should still be appropriate but the energy required to create new surfaces might be dependent on the rate of loading. This aspect needs to be investigated analytically or experimentally.

The problem of crack arrest is a transient dynamic phenomenon regardless of loading conditions. Consider the dynamic crack propagation process initiated by a quasi-static loading process, the crack initiation can occur mainly in a quasi-static stress state but the

subsequent growth takes place in a dynamic stress field. Considerable experimental work has been performed on the problem of crack arrest, particularly in structural steel. The existence of a critical stress-intensity factor at which the crack comes to stop is still debated. A deceleration prior to crack arrest was observed by some [Kalthoff, 1977]; others noted an abrupt arrest [Schardin, 1959]. A possible reason for some confusion on this topic is that experiments are typically conducted upon relatively small specimens and the presence of wave reflections and interactions lead to a very complicated stress histories at the crack-tip.

Between crack initiation and crack arrest crack travels at a high velocity governed by the applied loading and the material properties. Schardin [1959] determined that cracks in glass as well as plexiglass travelled with a constant maximum velocity. Theoretical calculations based on the elasto-dynamic stress field have led to the conclusion that the Rayleigh wave speed sets a limit on the velocity with which a crack may propagate [Freund, 1972]. However, experimentally obtained maximum velocities are much lower, being typically around 50 percent of the Rayleigh wave speed. Much of experimental work [Irwin, 1979, Kobayashi, 1978 and Kobayashi and Dally, 1977 and Dally et al., 1985] on crack propagation has concentrated on determining the relationship between the applied loading, expressed in terms stress intensity factor, and the response of the crack, as determined by the instantaneous crack velocity. There is a wide discrepancy between the above experimental observations and theoretical calculations based on the energy balance equations. In all the above studies, a large part of this discrepancy is due to the idealization of crack growth as the propagation of sharp plane crack.

Schardin [1959] demonstrated that when the applied loading is high, propagating cracks in glass specimens had a tendency to branch into two cracks. Since then other researchers have demonstrated crack branching in many materials, both crystalline and amorphous [Field, 1971, Finkel, 1963]. However, to date there exist no satisfactory explanation of the mechanism that causes propagating cracks to branch. Ravi Chander et.al. [1984c] used microstructural viewpoint of crack propagation to arrive at a mechanism crack propagation that treats crack branching as a continuum evolution within the fracture process

zone at the front of the crack. They have found that a typical dependance of critical crack size on pulse amplitude exists regardless of the test material and that this dependance deviates in a typical and consistent way from what quasi-static prediction would yield.

Schardin [1959] and other investigators have observed crack branching in crystalline as well as amorphous materials. This phenomenon has not been explained by analytical means although notable attempts have been made by Achenbach [1975], Dempsey and Burgers [1982].

Yoffe [1951] attempted to explain branching of cracks from an analysis of the problem of cracks of constant length that translates with a constant velocity in an unbounded medium. This work was the first attempt to study the dynamic stress field around a moving crack-tip and proposed a peak circumferential stress criterion for branching.

Eshelby [1970] approached the branching problem from the viewpoint of energy balance. It is known that the dynamic energy release rate G can be expressed as $G = G^* g(v)$, where G^* is the dependent on the geometry and loading $g(v)$ as the velocity dependent function and it is approximated by $g(v) = 1 - V/C^r$, where C^r is the Rayleigh wave Speed. V is the velocity of propagating crack. Since after branching two cracks are created, the crack will not propagate unless the velocity factor g(v) is doubled with a corresponding reduction on crack speed. From the above equation one can deduce that in order for the factor g(v) to double, the velocity before branching must be greater than $0.5\, C^r$ and it must drop upon branching. Another attempt to make crack branching plausible rests on stress wave hypothesis [Lawn and Wilshaw, 1975].

The angle between branches is fairly well predicted by Kalthoff [1971] from the considerations of bimodal crack growth. When the crack deviates from the plane perpendicular to the tensile stress it is also subjected to shear stresses, i.e., $K_{II} \neq 0$. The behavior of crack ~~of crack~~ under combined K_I and K_{II} conditions are treated.

Shukla and Anand [1986] carried out study of the crack propagation and branching under biaxial loading. They concluded that the branching stress intensity factor and the crack velocity showed relatively no dependence on the nature of the remote parallel stress within the normal and vertical stress ratios and experimental results indicated that any criterion predicting crack branching angle must take the sign of the far field stress.

Clark and Irwin [1966] proposed that the dynamic stress intensity factor should reach a critical value K_{Ib} for branching to occur at a terminal velocity. Kobayashi [1974] used photoelasticity techniques to determine the dynamic stress intensity factors and proposed that crack branches when it reaches a terminal velocity. Ramulu and Kobayashi [1984] have utilized the directional instability of a running crack in conjunction with the crack-tip micro-cracking concepts. Sih [1977] and Theocaris [1985] have approached the problem using the concepts of strain energy density. Branching phenomenon has been related to the fracture surface topography and surface roughness by Ravi Chander and Knauss [1984a, 1984c]. Shukla et. al [1989] have proposed a another criterion by modifying the Theocaris criterion which predicts that an increase in the remote parallel stress lead to increase in branching angle.

To date published analytical attempts at clarifying crack branching have all been directed to seek necessary condition for branching through a comparison of stress states prior to and after crack branching. The stress state after branching as obtained via the following assumptions: A fast running crack comes to rest abruptly. In doing so it radiates an appropriate stress field in which two branches emanate instantaneously from the stopped crack at some arbitrary angles but symmetrically with respect to original crack.

1.2 OBJECTIVE OF THE PRESENT WORK

From a critical review of the available literature, it is felt that there is a need to study and understand the high speed crack propagation and branching through a hybrid experimental-numerical approach. However, since the numerical dynamic fracture simulations require

experimentally measured information as the input data some experimental techniques have been devised to record the crack propagation history.

With this in view, in this present work an efficient finite element model has been developed to study the linear elasto-dynamic crack propagation and branching in isotropic solids as well as orthotropic composite materials. Stationary mesh procedures are used in the generation phase simulation in which the variation of fracture toughness ($\hat{J}_1$-integral) is determined using the experimentally determined crack-propagation history. The experiments are designed such that the crack initiation takes place in a quasi-static stress state and consequent crack growth occurs in a dynamic stress field. The crack propagation history is recorded using a propagation gauges and associated electronic circuit [Ray, 1994]. The study is conducted on specimens made of PMMA as it is easily available.

1.3 LAYOUT OF THE THESIS

The present work attempts to understand the high speed crack propagation and branching in PMMA specimens.

Chapter II of the thesis gives the fundamentals of linear-elasto-dynamics, Finite Element Modelling of dynamic propagation and branching, spatial and temporal discretizations and the details of computer implementation.

Chapter III describes the experimental technique adopted and experimental details of recording the crack-propagation history. The procedure to obtain the crack branching is also discussed in detail.

Chapter IV gives the results and discussions of the investigation using the hybrid experimental and Finite Element approach.

Chapter V gives the conclusions and scope for further work.

CHAPTER 2

FINITE ELEMENT MODELLING OF CRACK PROPAGATION AND BRANCHING

This chapter describes the fundamentals of the theory of linear elasto-dynamic crack propagation and the finite element formulations of the governing hyperbolic partial differential equations. The spatial and temporal descretizations, the time integration, stability of the algorithm are also discussed. The computational simulation of the moving crack is discussed in detail.

2.1 THEORY OF LINEAR ELASTO-DYNAMICS

The theory of linear elasto-dynamics is embodied in the following set of equations defined for a body of volume V enclosed by surface $S = S_1 + S_2$, where on S_1 the displacements are specified and on S_2 the tractions are specified (Fig. 2.1).
Equations of motion are given by :

$$\nabla . \tau + \rho \bar{f} = \rho \frac{\partial^2 \bar{u}}{\partial t^2} \qquad (2.1)$$

where τ is the stress tensor, $\bar{u}$ is the displacement vector, $\bar{f}$ is the body force vector per unit volume and ρ is the mass of the material.
The constitutive equations are:

$$\tau_{ij} = C_{ijkl} \left(\frac{\partial u_l}{\partial x_k} \right) \qquad \bar{x} \ in \ V \qquad (2.2)$$

where C_{ijkl} are the elastic stiffnesses.

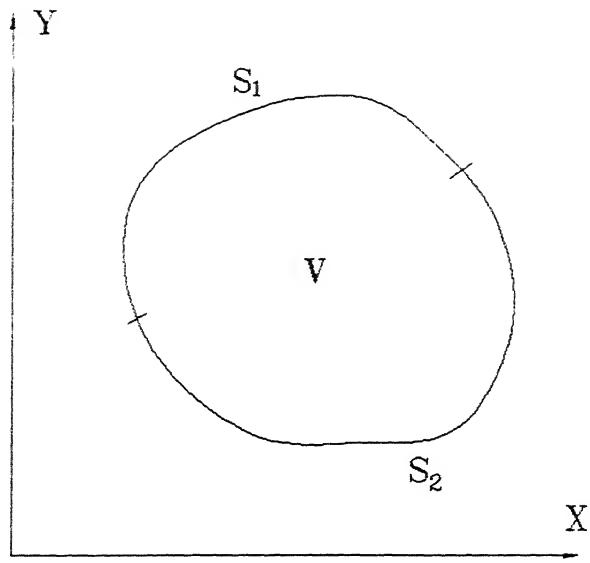

Fig. 2.1 Generalized body

The boundary conditions are:

$$\begin{aligned} \bar{u}(\bar{x},t) &= \bar{U} \qquad \bar{x} \text{ on } S_1 \text{ (Displacement B.C)} \\ \bar{n}.\tau(\bar{x},t) &= \bar{T} \qquad \bar{x} \text{ on } S_2 \text{ (Traction B.x} \end{aligned} \tag{2.3}$$

The initial conditions are

$$\begin{aligned} \bar{u}(x,0) &= \overline{u_0} \\ \bar{u}(x,0) &= \overline{v_0} \qquad x \text{ in } V \end{aligned} \tag{2.4}$$

where $\overline{u_0}$, $\overline{v_0}$, $\overline{U}$, $\overline{T}$ are the prescribed quantities.
Eqs 2.1 and 2.2 can be combined into one vector equation for $\bar{u}(x,t)$,

$$\frac{\partial}{\partial x_j}\left(C_{ijkl}\frac{\partial \overline{u_j}}{\partial x_k}\right) + \rho f_i = \frac{\partial^2 \overline{u_i}}{\partial t^2} \tag{2.5}$$

This is the Navier-Cauchy equation of motion for anisotropic inhomogeneous elastic solids.

The total potential of a linear elastic body, neglecting body forces can be give by D' Alembert's principle as

$$\pi = \int_v u_{i,j}\tau_{i,j}dV - \int_s u_i \quad t_i \, ds + \int_v u_i \rho \ddot{u}_i \, dV \tag{2.6}$$

where the first term is the strain energy, second term is the work done by the surface traction vector and the last term is the work done by the inertia forces. The integrations are carried out over the volume of the body V or surface s, whichever is applicable.

The finite element formulations involve the descretization of the domain into suitable elements, approximation of the field variables interior to the elements in terms of their nodal values through the shape functions of the chosen element and the determination of nodal values through the minimization of the above energy functional. Invoking the

stationarity of π, namely, $\delta\pi = 0$, the following equation may be obtained.

$$\int_v \delta u_{i,j}\tau_{i,j}\, dV - \int_s \delta u_i t_i\, ds + \int_v \delta u_i \rho u_i\, dV = 0 \qquad (2.7)$$

Approximating the field values (u) within the element in terms of its nodal values as

$$u^e(x,y,z,t) = N^e(x,y,z,t)U^e(t) \qquad (2.8)$$

From this the following strain-displacement relation is obtained.

$$\varepsilon^e(x,y,z,t) = B^e(x,y,z,t)\ U^e(t) \qquad (2.9)$$

The constitutive equation is

$$\tau^e(x,y,z,t) = D^e\varepsilon^e(x,y,z,t) \qquad (2.10)$$

N^e is the displacement interpolation matrix, B^e is the strain-displacement matrix and D^e is the material property matrix.

Substitution of Eqs 2.8 through 2.10 in Eq. 2.7 gives the equation of motion in the matrix form as,

$$[M]\left[\frac{\partial^2 U}{\partial t^2}\right] + [K]\,[U] = [F] \qquad (2.11)$$

where

$$\begin{aligned}
[M] &= \sum [M]^e, \\
[K] &= \sum [K]^e, \\
[F] &= \sum [F]^e, \\
[M]^e &= \int_{V_e} \rho\,[N]^T[N]\ dV, \\
[K]^e &= \int_{V_e} [B]^T[D]\,[B]\ dV, \\
[F]^e &= \int_{S_e} [N]\ [t]\ ds.
\end{aligned} \qquad (2.12)$$

The Eq.2.11 may be solved by several methods. In the present work Newmark's average acceleration scheme and scheme have been used. The Newmark method is discussed in Sec. 2.5.

2.2 BASICS OF DYNAMIC FRACTURE

In linear elasto-dynamic fracture mechanics, the conditions governing the crack can be expressed in an analogous way to that of the static fracture. The dynamic stress intensity factor is generally a function of crack length a, applied load σ and time t. In the generalization of linear elastic fracture mechanics (LEFM), to dynamic fracture there are two types of critical material parameters. First, for the initiation of crack growth under dynamic loading

$$K(a, \sigma, t) = K_d(\dot{\sigma}) \qquad (2.13)$$

where K_d is the dynamic initiation toughness and depends on the loading rate. When quasi-static condition prevail in the material, under LEFM considerations, K_d reduces to quasi-static initiation fracture toughness K_c. Secondly, for propagating crack

$$K(a, \sigma, t) = K_D(\dot{a}) \qquad (2.14)$$

where K_D is the dynamic propagation toughness and depends on the crack velocity. Eq. 2.13 and 2.14 may also be expressed in terms of G. Since a computational model gives solutions to the prescribed input data, numerical simulations of dynamic fracture in a material require experimentally measured information as input data. Thus, the present approach is labelled as the *hybrid experimental-numerical method.* Computational simulations of dynamic crack propagation and crack arrest, for a specified specimen geometry and applied load can be conducted in either of the two different ways. The first of these is called *Generation phase simulation* in which variation of stress intensity factor (and/or energy release rate) can be determined using experimentally measured crack propagation and loading history as the input data into the computational model. From this calculation, one can determine initiation and propagation toughnesses.

Secondly, if the material properties K_d and K_D are determined either numerically or experimentally, they may be used in a *Prediction phase simulation.* In this calculation, the propagation history can be determined by specifying the initial conditions and material fracture toughness data as the inputs to the model.

A generation phase simulation is used in this investigation to simulate the dynamically propagating crack computationally and to arrive at the values of the K_D and K_d. The determination of crack propagation history is discussed in the chapter III.

2.3 MODELLING OF CRACK PROPAGATION AND BRANCHING

To simulate crack propagation in solids, two different concepts of computational modelling are in use i.e, *stationary mesh procedure* and *moving mesh procedure* [Nishioka and Atluri, 1986]. In this investigation stationary mesh procedure with linear relaxation of the holding back force on the crack tip node is employed. Double nodes are used on the crack path nodes as well as on the two branches of the branched crack. A triple node is used at the point of crack bifurcation as shown in the Fig. 2.2.

When the material is uncracked (crack in not propagated upto that node), the triple nodes and the double nodes are combined to form a single node by imposing the condition:

$$\begin{aligned} &u_i = u_j \\ &f_i + f_j = o \end{aligned} \quad \text{for a double node } (i,j)$$

$$\begin{aligned} &u_l = u_m = u_n \\ &f_l + f_m + f_n = o \end{aligned} \quad \text{for a triple node } (l,m,n) \qquad . \quad (2.15)$$

where u is the displacement and f is the resultant force at that particular node.

When the crack at a particular double node or a triple node is present the corresponding double node or the triple node is set free.

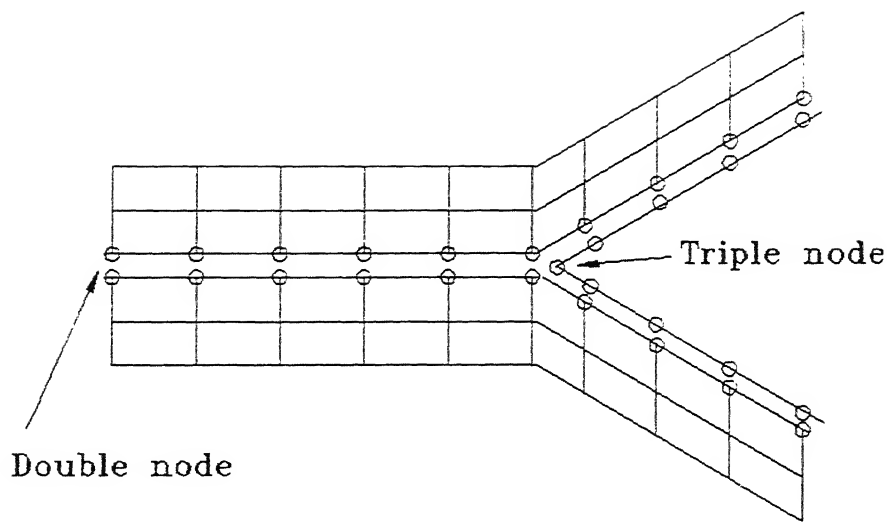

Fig. 2.2 Computational modelling of crack propagation and branching

The $\hat{J}_1$ is defined with the assumption that crack is not kinking or is not abruptly changing the direction and velocity of propagation. Thus $\hat{J}_1$ is not defined after the crack branching. However, the value of dynamic energy release rate in mode-I and mode-II can be calculated at the instance of release of the double nodes after the branching. The holding back force and the displacement at the double nodes are transformed at half of the branching angle (Fig. 2.3) and the dynamic energy release rate in mode-I and mode-II can be calculated by using the Eq. 2.16.

$$G_I = \frac{1}{2} F_I U_I$$
$$G_{II} = \frac{1}{2} F_{II} U_{II} \qquad (2.16)$$

where F_I and F_{II} are the transformed holding back forces and U_I and U_{II} are the distances between the two double nodes in normal and parallel directions respectively.

2.3.1 Stationary Mesh Procedure

Usually finite element equations for the stationary mesh procedures are derived based on the standard principles of virtual work. For a linear elastic material undergoing infinitesimal deformation, the equations of motion for the finite element model can be given by 2.11. This system of equations can be solved either by time integration or by mode superposition method, of which the former method is preferred in the wave propagation problems due to its simplicity. For time integration there are many schemes. The Newmark's average acceleration scheme is used in the present study. In the stationary mesh procedure of modelling linear elasto-dynamic crack propagation, when the node spacing is $C\Delta t$ (C being the crack velocity), one has to release the constraint on the old crack-tip node. This is known as the simple node-shifting procedure. In this procedure the sudden increase in the crack length and the release of the constraint on the displacements on the old crack-tip node induce spurious high-frequency oscillations in the finite element solutions. To overcome these difficulties the nodes are released gradually, over a finite period of time.

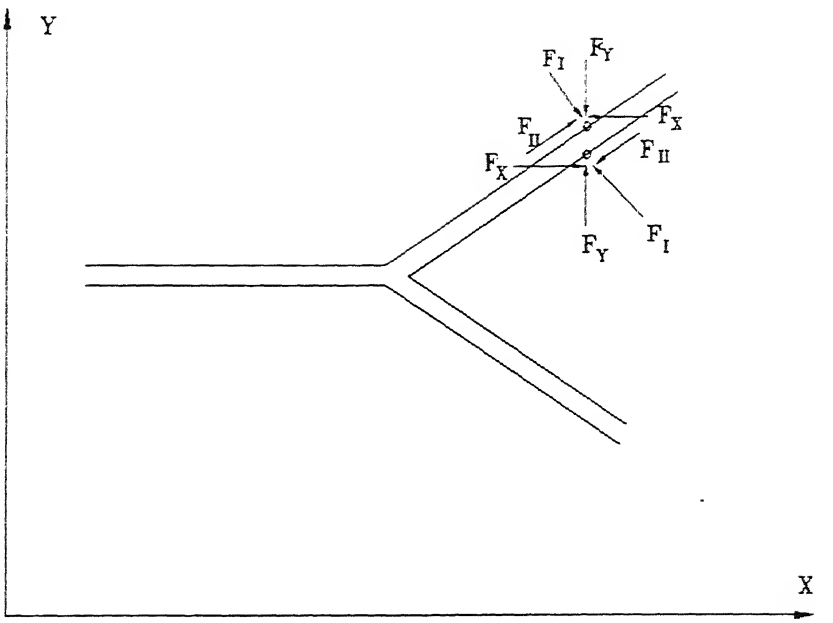

Fig. 2.3 Holding back forces on the double node

Several gradual nodal release mechanisms were presented in the literature, with different rates of release of nodal forces. Suppose that the actual crack-tip is located at point C in between the finite element nodes B and D as shown in the Fig. 2.4. b and d are the lengths of segments BC and BD respectively. The holding-back force F at node B is gradually released to zero as the crack tip reaches the node D. The various schemes for accomplishing this are summarized below.

Malluk and King[1978] $F/F_o = (1 - b/d)^{1/2}$ (2.17a)

Rydholm et al.[1978] $F/F_o = (1 - b/d)^{3/2}$ (2.17b)

Kobayashi et al.[1978] $F/F_o = (1 - b/d)$ (2.17c)

where F_o is the original reaction force when the crack-tip is located at the node B. It is important to recognize that the crack-tip movement from B to D takes place in several time-steps of Δt. The Eqs.(2.17a,b) are derived by assuming constant stress-intensity factor and a constant energy release rate, respectively, during the time between the nodes B and D. The Eq.(2.17c) is based on pure intuition. However, since the linear relaxation technique, which is most simple to implement, is recommended in the literature, the present study makes use this technique.

2.4 SPATIAL AND TEMPORAL DESCRETIZATION

For wave propagation problems low-order elements and uniform meshes are recommended [Bathe, 1982]. Hence bilinear quadrilateral isoparametric elements have been used. The shape functions and the derivatives of the bilinear isoparametric element are given in Appendix-A. In this investigation, a typical spatial descretization of 2880 elements is used. The total number of the nodes depends on the number of the double nodes and the triple nodes.

The system of linear, second order, ordinary differential equations with constant coefficients has been integrated by discretizing the time variable as $t_n = n\ \Delta t$, $0 \le n \le N$.

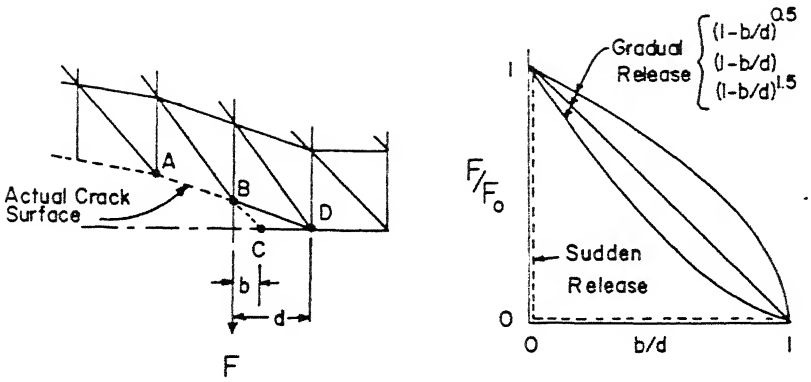

Fig.2.4 Gradual node release techniques

2.5 NEWMARK'S METHOD

The Newmark's constant-average acceleration scheme makes the following assumptions.

$$\frac{\partial U^{t+\Delta t}}{\partial t} = \frac{\partial U^{t}}{\partial t} + \left[(1-\delta) \frac{\partial^2 U^{t}}{\partial t^2} + \delta \frac{\partial^2 U^{t+\Delta t}}{\partial t^2} \right] \Delta t$$

$$U^{t+\Delta t} = U^{t} + \frac{\partial U^{t}}{\partial t} \Delta t + \left[\left(\frac{1}{2} - \alpha \right) \frac{\partial^2 U^{t}}{\partial t^2} + \alpha^{t+\Delta t} \frac{\partial^2 U}{\partial t^2} \right] \Delta t^2 \qquad (2.18)$$

where α and δ are parameters that can be determined to obtain integration accuracy and stability. Newmark [Newmark, 1959] originally proposed an unconditionally stable scheme known as the constant average acceleration method, in which $\alpha = 0.25$ and $\delta = 0.5$. In addition to the above difference equations, for solution of displacements, velocities and accelerations, the equilibrium equations at time $t+\Delta t$ are considered.

$$M^{t+\Delta t} \frac{\partial^2 U}{\partial t^2} + K^{t+\Delta t} U = F^{t+\Delta t} \qquad (2.19)$$

Using Eqs. 2.11 and 2.12 the following equation can be obtained.

$$\left(M + \frac{\Delta t^2}{4} K \right) U^{t+\Delta t} = \frac{\Delta t^2}{4} F + M \left(U^{t} + \Delta t \frac{\partial U^{t}}{\partial t} + \frac{\Delta t^2}{4} \frac{\partial^2 U}{\partial t^2} \right) \qquad (2.20)$$

2.6 BOUNDARY AND INITIAL CONDITIONS

In the simulation of dynamic crack propagation studied in this investigation, the plate is loaded by applying a known edge displacement prior to the crack initiation and the subsequent crack growth takes in dynamic stress field. The far field displacement is applied on the boundaries as the boundary condition and the initial conditions are:

$$U^{o} = 0; \quad U^{-\Delta t} = 0; \quad \frac{\partial U^{o}}{\partial t} = 0 \qquad (2.21)$$

2.7 ERROR AND STABILITY CONSIDERATIONS

One important criterion for an accurate solution of the problem is the choice of the time step Δt for the time integration. A larger time step is preferred for the computational economy; whereas a small value is required for convergency. An optimum choice of time step is generally considered to be $\Delta t = d/c_d$ [Harzman and Hutchinson, 1972] in which d is the smallest mesh size and c_d is the dilateral wave velocity. In general the velocity of crack propagation is significantly lower than the wave velocity, the crack-tip, during this time increment Δt, will move to a position in between the nodal points, assuming that the crack-tip is coincided with a node at time $t-\Delta t$.

2.8 CALCULATION OF $\hat{J}_1$-INTEGRAL

It is well known that in mode-1 elasto-static fracture, the so called J-integral can be used for efficient and simple computation of relevant crack tip parameters. This is so because, under appropriate assumptions of material homogeneity, etc., the strength as the crack-tip fields (K_I for instance) is governed by an integral evaluated over a path that is far away from the crack-tip. The far field integral can be evaluated with reasonable accuracy using relatively coarse finite element meshes.

Out of several path-independent integrals given in literature, [Kishmoto et al., 1980 and Atluri [1982]), $\hat{J}_k$ given by Kishomoto et al. is used in the present work. This is an inertia enhanced version of J-integral defined by Rice [1968].

The $\hat{J}_k$ is defined as follows (Fig. 2.5);

$$\hat{J}_k = \lim_{\epsilon \to 0} \int_{\Gamma_\epsilon} [\, W n_k - T_i u_{i,k} \,]\, dS - \lim_{\epsilon \to 0} \left(\int_{\Gamma + \Gamma_\epsilon} [\, W n_k - T_i u_{i,k} \,] dS + \int_{V_\Gamma + V_\epsilon} \rho \ddot{u}_i u_{i,k}\, dV \right) \tag{2.22}$$

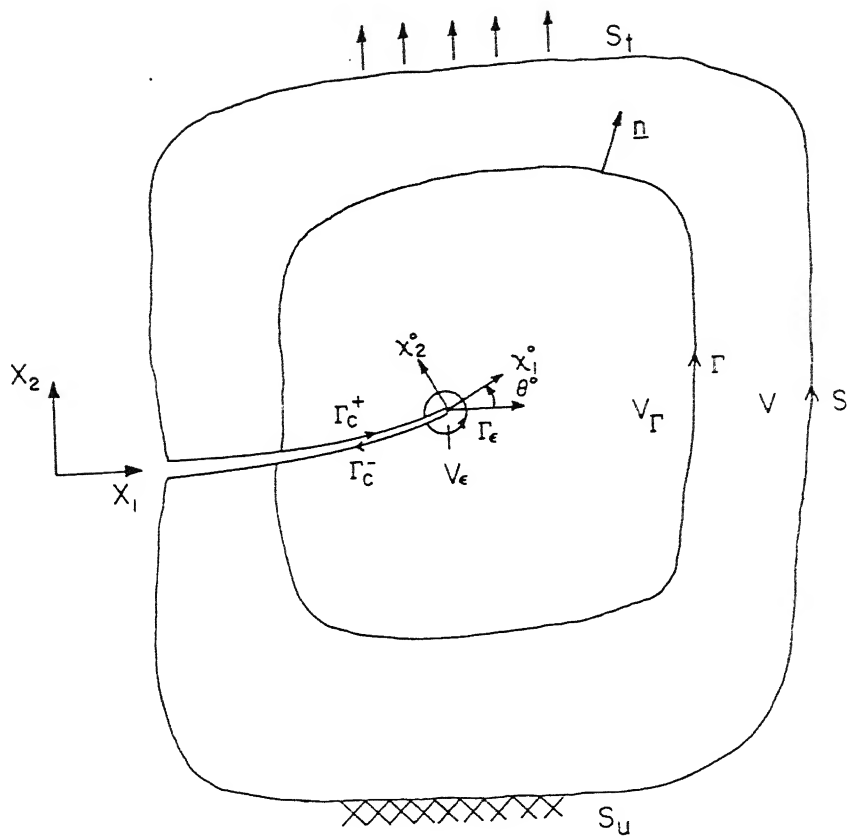

Fig. 2.5 Contours for path-independent integrals

2.9 COMPUTER IMPLEMENTATION

The two dimensional finite element code developed to model linear elasto-dynamic crack propagation can be used for homogeneous elastic as well as orthotropic solids [Jaleel, 1992]. The computer code is in three parts: a pre-processor, a processor and a post- processor.

The pre-processor consists of a computer code in FORTRAN-77 to generate the nodal coordinates and nodal connectivity for quadrilateral elements used, and a menu based graphics program to draw the mesh using these coordinates and the nodal connectivity. For verification purposes, the code can also zoom a particular portion of the mesh generated.

The processor is the main body of the package and consists of a computer code in FORTRAN-77 to model linear elasto-dynamic crack propagation. The storage scheme used is the compressed skyline-storage method [Felippa, 1973]. This allowed modelling of fairly large domains. The Finite Element Equations are solved using cholesky decomposition.

The post-processor consists of a code for drawing the deformed mesh configurations.

CHAPTER 3

EXPERIMENTAL TECHNIQUE

This chapter describes the details of the experimental methods adopted to produce a high static load prior to the crack initiation and the technique to measure the load and crack propagation history.

3.1 EXPERIMENTAL DETAILS

As mentioned in Sec 1.3, the specimen in the present study, is subjected to a quasi-static loading prior to the crack initiation to store a high static energy. For this purpose, a loading frame is designed and manufactured in the ESA laboratory, to load the specimen in a displacement controlled mode. The drawing of the loading frame is shown in the Fig. 3.1. The crack propagation velocity is measured by means of crack propagation gauges and a necessary electronic circuit. The far field strain as a function of time is measured using four channel differential storage oscilloscope (GOULD). As the total number of the channels present in the oscilloscope are four, two strain gauges are mounted on the specimen to record the far field strain, a crack propagation gauge to measure the crack-tip location as a function of time and one more strain gauge near the crack-tip is used as a crack propagation gauge. The strain gauge near the crack tip is mounted at an angle of approximately to record a peak whenever the crack-tip passes by it. The time instance at which the voltage peak has occurred and the distance of the strain gauge from the initial crack-tip position are used in the calculation of the crack propagation speed. The velocity of the crack propagation and the far field strains can be estimated by the analysis oscilloscope records.

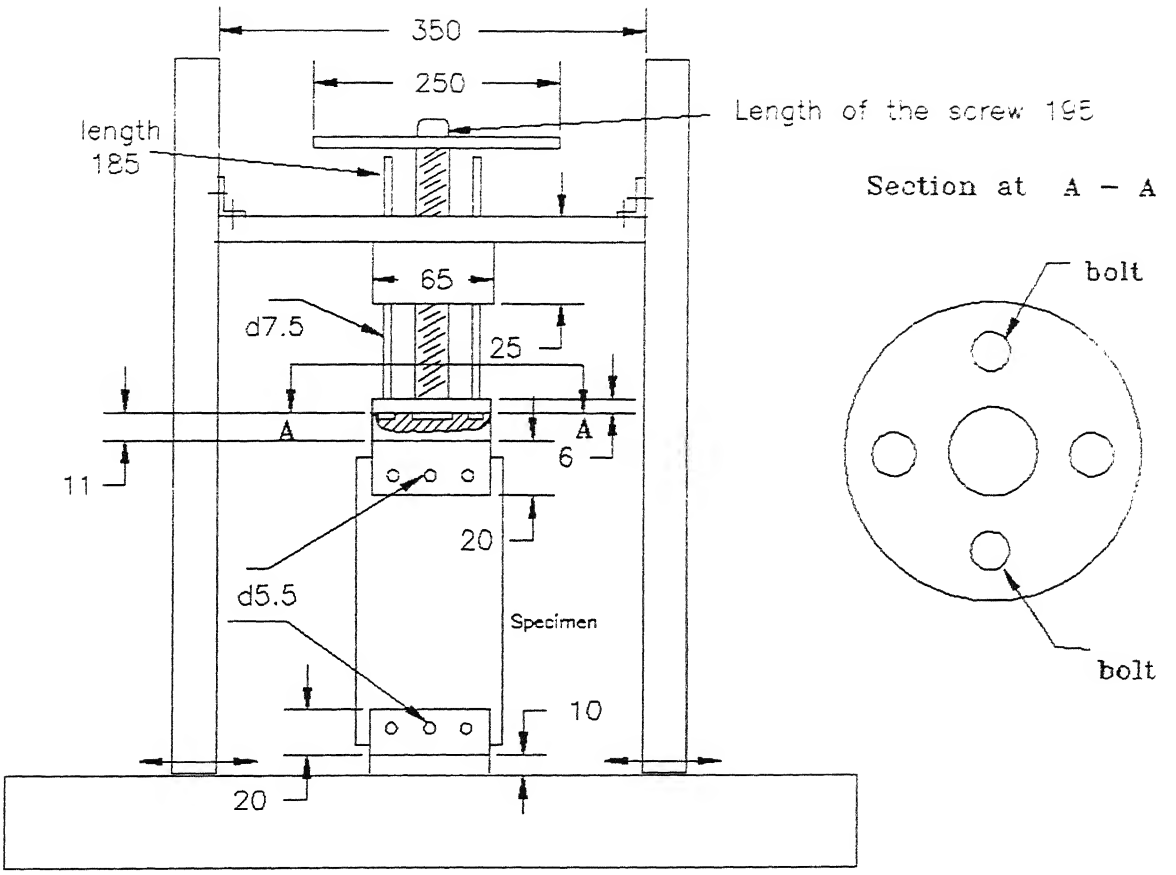

Fig. 3.1 Loading Frame

3.2 MEASUREMENT OF CRACK PROPAGATION SPEED

Four thin strips of aluminum foil which are connected at one end and free at the other end are pasted to the specimen. The free ends of the strips are connected to the electronic circuit unit (Fig 3.2). The strips are numbered 1, 2, 3 and 4. with the strip 1 being the one on crack-tip. The distance between the strips are carefully measured. The electronic circuit produces a voltage drop whenever any aluminum foil breaks. The voltage drop is recorded on the oscilloscope as a function of time. Since shearing of the ductile aluminum foil takes some finite time when the crack propagates across it, the portion of the aluminum strips in the vicinity of the crack-tip is replaced by a silver paint coating. The silver paint breaks as soon as the crack propagates under it thereby producing immediate voltage drop. The schematic diagram of the aluminum foils pasted to the specimen is shown in Fig. 3.3. The magnitude of the voltage drop so produced is different for each strip and the ratio of the magnitudes of the voltage drop for strips 1, 2, 3, 4 is 8:4:2:1 with the magnitude of voltage drop for strip 1 being 800 mV. Knowing the distance between the strips and the time at which the drops occurred the velocity of the crack can be calculated.

3.3 EXPERIMENTAL PROCEDURE

The PMMA specimen of 200 mm x 125 mm of 2 mm thickness are used to conduct the study. The specimens are prepared with an initial crack of $a/w = 0.25$, where a is crack length and w is the width of the specimen, with a fine hole drilled ahead of the crack-tip. The hole is drilled with an aim to make the crack blunt thereby storing a high static elastic energy before the crack initiates. The intention behind this is that when the crack initiates under a load of 2 to 3 times the critical load, it starts releasing the energy at a faster rate (i.e, the crack moves with a much higher velocity). When this energy is sufficient to propagate two cracks, the crack branches. This is checked with a trial experiment wherein the specimen was loaded to a load of about 2.78 times critical load. After the propagation of one crack for about 5 cm the branching was observed and the branching angle was found to be approximately 25°.

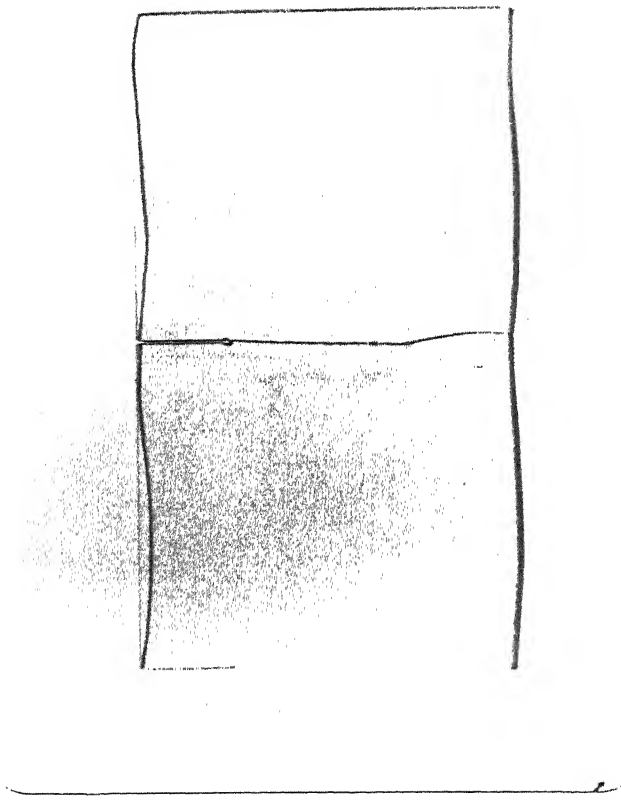

Photograph showing the fractured specimen in the trial experiment

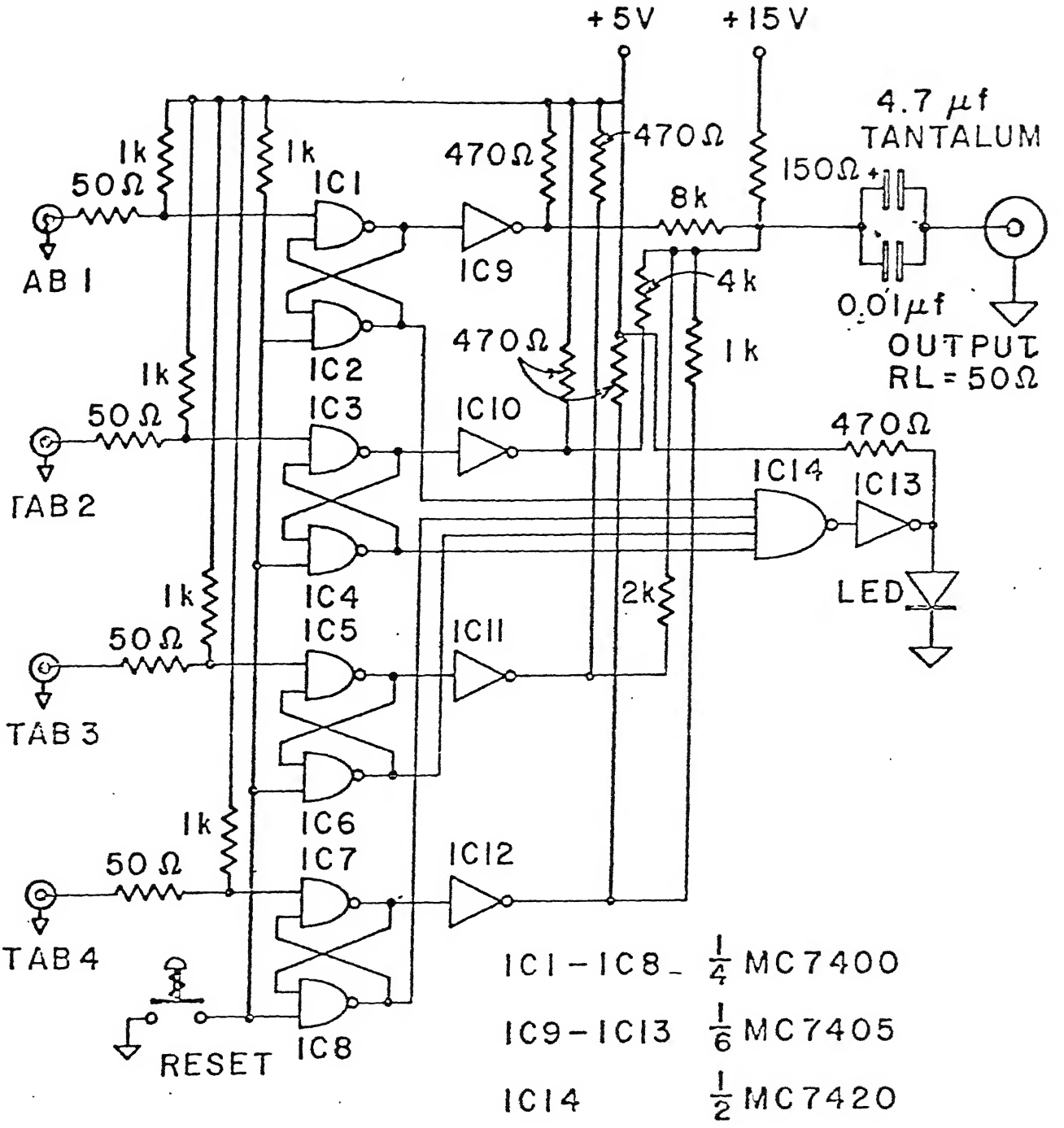

Fig. 3.2 Electronic circuit for propagation gauges

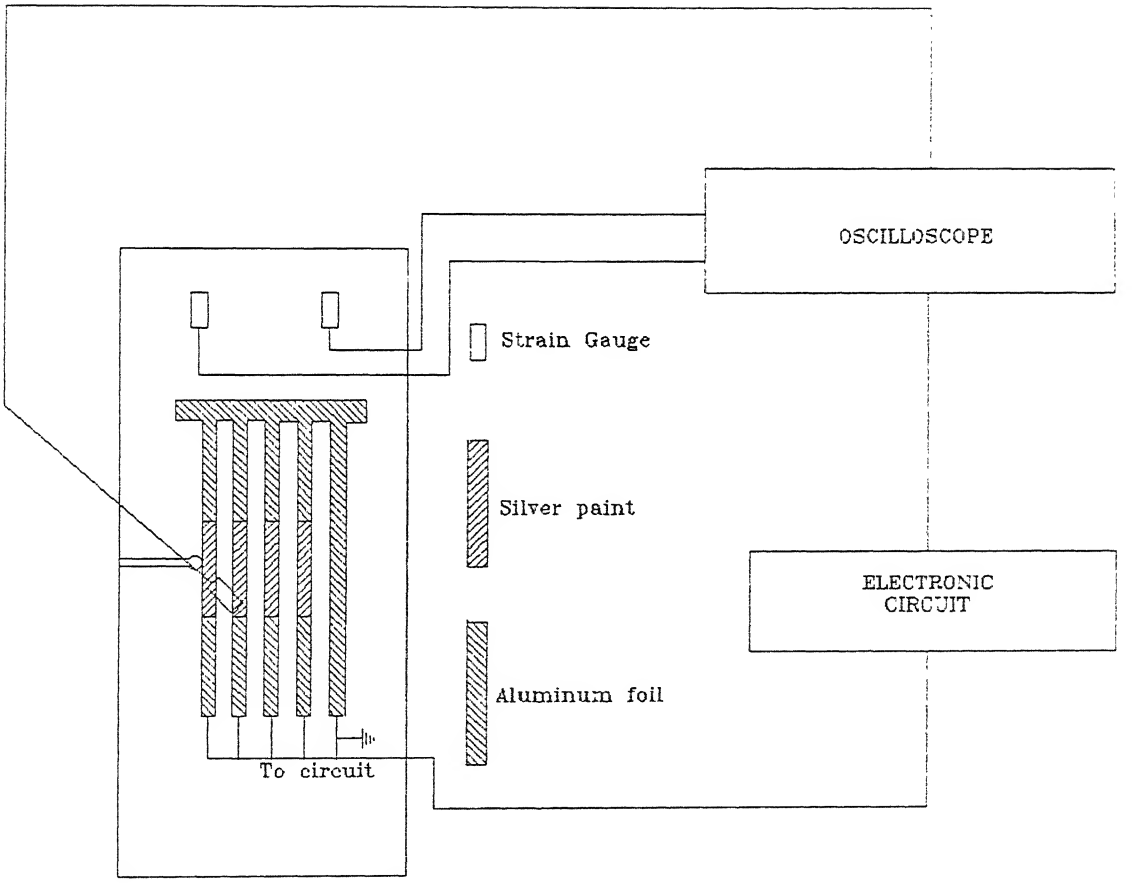

Fig. 3.3 Schematic diagram of the specimen

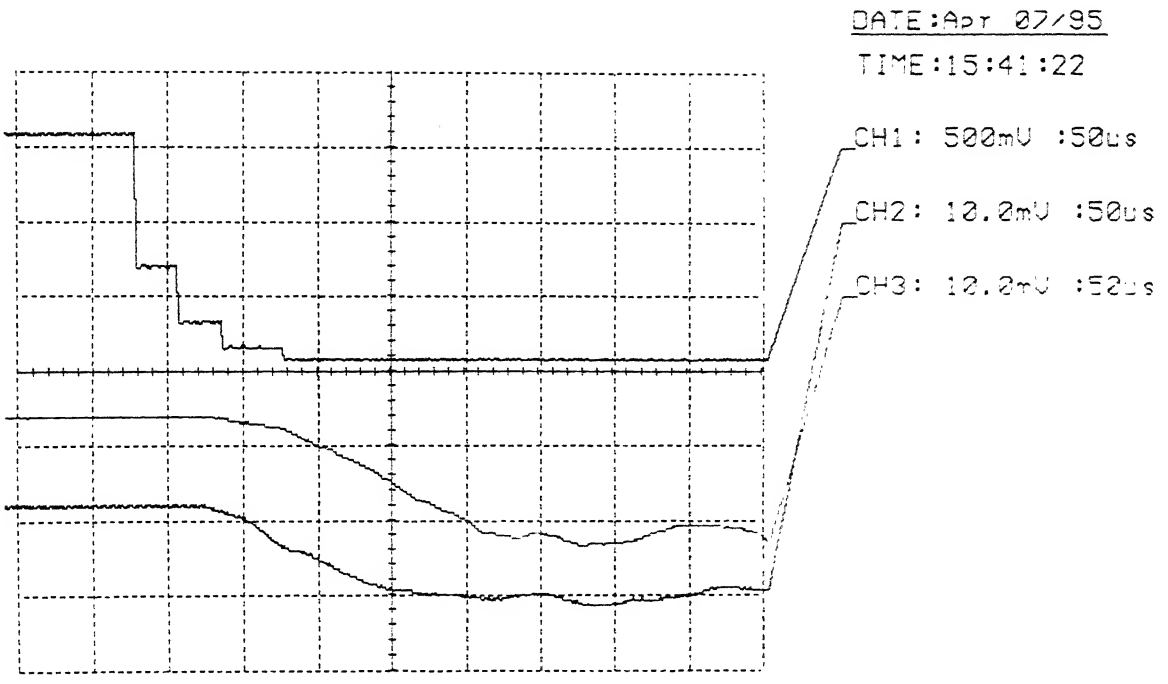

Fig. 3.4 Typical record of the oscilloscope

Two strain gauges are mounted on the specimen to measure the far field strain and another strain gauge is mounted near the crack-tip to use as a crack propagation gauge. The record of the oscilloscope is shown in Fig. 3.4 for a typical experiment. The records of the oscilloscope show the voltage drops Vs time produced by the electronic circuit and the far field strain Vs time.

The variation of far field strain and crack-tip location with time are used in crack propagation simulation by FEM as described in chapter 2 to arrive at the initiation and propagation fracture toughnesses. The results of several experiments are described in chapter 4.

CHAPTER 4

RESULTS AND DISCUSSION

In this chapter results of the various experiments performed and the corresponding numerical modelling of crack propagation are discussed.

As explained in earlier chapters, the numerical modelling of the crack propagation and branching requires the following inputs.

- The crack propagation history i.e the crack-tip location as a function of time.
- The displacement at the gripped ends of the specimen.

4.1 EXPERIMENTAL OBSERVATIONS

The specimen is pre-loaded in a displacement controlled mode prior to the crack initiation. The strain gauges mounted on the specimen at a distance of 85 mm from the crack-tip plane, record the far field strain as a function of time. The crack-tip position as a function of time is obtained from the oscilloscope record from the output of the crack propagation gauges and the electronic circuit. The crack-tip location is plotted as a function of time. The results of the various experiments performed are summarized in Table 4.1.

Experiment # 1 : Fig. 4.1a shows the traces oscilloscope record with the far field strain, the voltage drops produced by the electronic circuit and the strain recorded by the strain gauge mounted near the crack-tip as a function of time. Channel-1 shows the voltage drops produced by the propagation gauge electronic circuit, channel-2 shows the strain calibrated in terms of voltage at a distance of 11.5 mm from the initial crack tip position and channel-3 and channel-4 show the far field strain calibrated in terms of voltage as a function of time. The voltage peak is produced in channel-2 occurs when the crack tip passes by the strain

gauge. It can be seen from the output of the channel-1 of the Fig. 4.1a that, out of four voltage drops to be obtained only two voltage drops could be obtained in this experiment. Knowing the distance between the conducting strips, the distance of the strain gauge from the initial crack-tip position, the time instances at which the voltage drops have occurred from channel-1 and the time instance at which the voltage peak is produced by the strain gauge near crack-tip as explained in Sec.3.1, the crack-tip location as a function of time is plotted in Fig. 4.1b. This relation is observed to be linear. The velocity of crack propagation is obtained from the slope of this straight line and it is observed to be 512 m/s. No branching is observed in this case.

The same procedure as in the experiment # 1 is used to plot the crack-tip location as a function of time in all the following experiments.

Experiment # 2 : Fig. 4.2a shows the oscilloscope record. Channel-1 shows the voltage drops produced by the propagation gauge electronic circuit as a function of time, channel-2 and channel-3 show the far field strain calibrated in terms of voltage as a function of time and the channel-4 shows the strain calibrated in terms of voltage as a function of time recorded by the strain gauge on the crack path at a distance of 25.6 mm from the initial crack-tip position. Only three drops could be recorded in this case. The crack-tip location as a function of time is shown in Fig. 4.2b. The crack in this case travelled at a slightly higher velocity of 552 m/s. The crack path showed *tendency to branch* at several locations. However, crack branching is not seen in this case also.

Experiment # 3 : Fig. 4.3a shows the oscilloscope record. Channel-1 shows the voltage drops produced by the propagation gauge electronic circuit and channel-3 and channel-4 show the far field strain as a function of time. Only two voltage drops could be obtained in this case. A little higher load could be applied and branching is observed. The branching angle is measured to be 26°. The crack-tip location as a function of time is plotted in Fig. 4.3b. The crack propagated at a constant velocity of 566 m/s before branching. However, the velocity after branching could not be recorded. In this case, crack branching occurred early, viz., at

a distance of 12 mm from the initial crack-tip position.

Experiment # 4 : Fig. 4.4a shows the oscilloscope record. Channel-1 shows the out put of the propagation gauge electronic circuit, channel-2 shows the strain calibrated in terms of voltage recorded by the strain gauge near the crack-tip at a distance of 10.2 mm from the initial crack-tip position and channel-3 and channel-4 show the far field strain calibrated in terms of voltage as a function of time. Only one voltage drop could be obtained in this case. A still higher load could be applied and multiple crack branching is observed. The crack-tip location as a function of time is plotted in Fig. 4.4b. The crack propagated with a little higher velocity of 576 m/s compared to the previous case before the first branching. The velocity after the first branching could not be recorded. The fractured surface showed *tendency to branch* at several places before the first successful branching at an angle of 25° is observed. Further branching from one of the branches at an angle of 32° is also observed. In this case, branching did not occur too close to the initial crack-tip position. The crack propagated 26.5 mm from the initial crack-tip position prior to branching compared with 12 mm in the third experiment.

Fig. 4.5a and 4.5b show the photograph of the fractured specimens in experiments 3 and 4. The specimen in Expt. # 3 has a clear branching at one location whereas the specimen in Expt. # 4 has several incipient branches before first significant branching.

4.2 NUMERICAL MODELLING

The preceding experimental data is used as the input to the FE modeling of crack propagation. The pre-loading on the specimen is prescribed as an equivalent displacement boundary condition and the corresponding static displacement field is imposed on the specimen at the start of first iteration of dynamic analysis.

The FE analysis is done in two stages. In the first stage, the analysis is done for a static case. The uniform edge displacement boundary condition is arrived at in this analysis

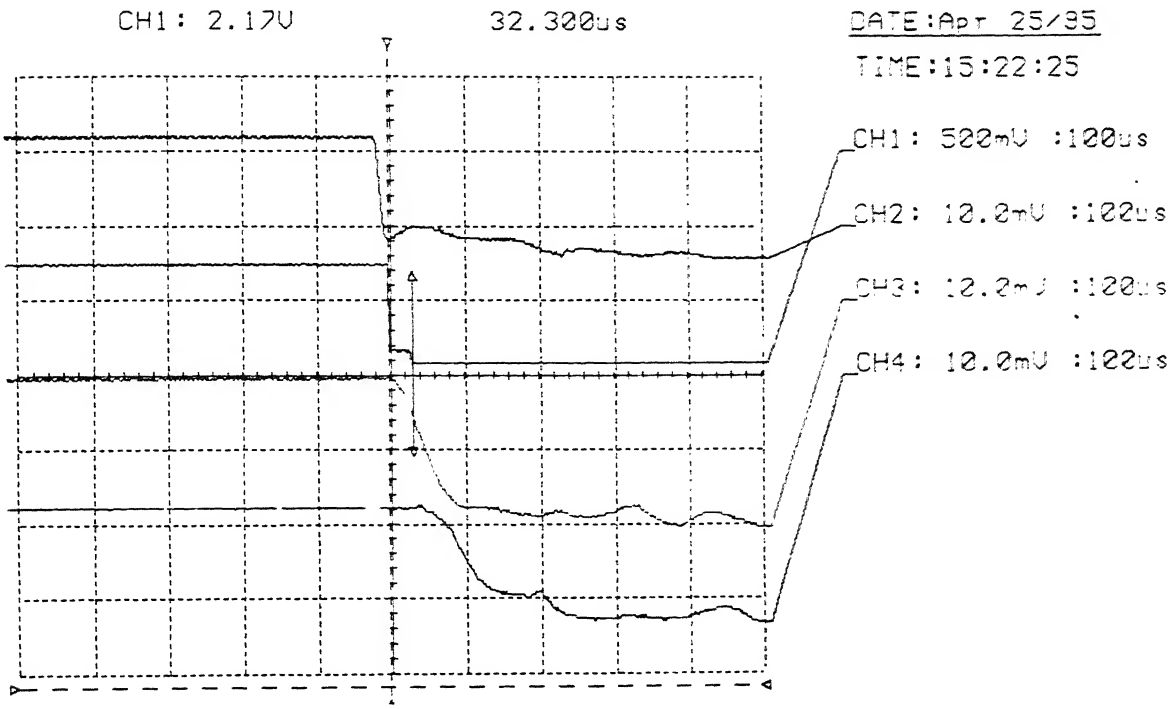

Fig.4.1a Oscilloscope record for Experiment # 1

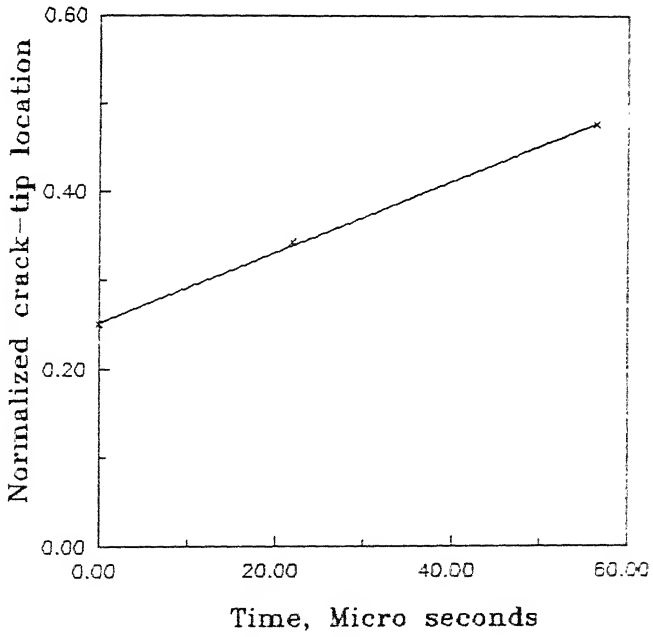

Fig. 4.1b Crack tip location as a function of time for Expt. # 1

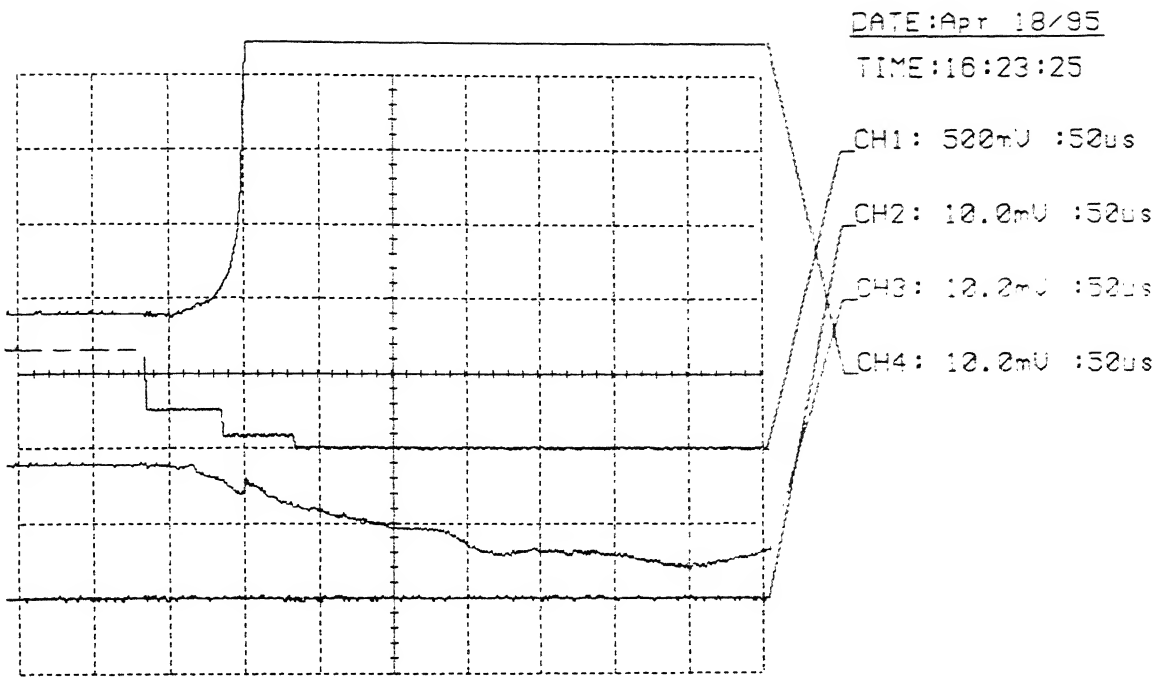

Fig. 4.2a Oscilloscope record for Expt. # 2

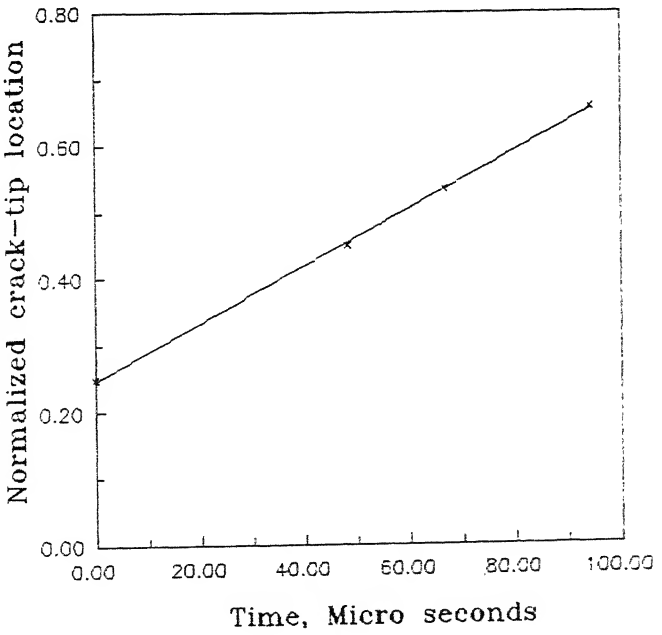

Fig. 4.2b Crack tip location as a function of time for Expt. # 2

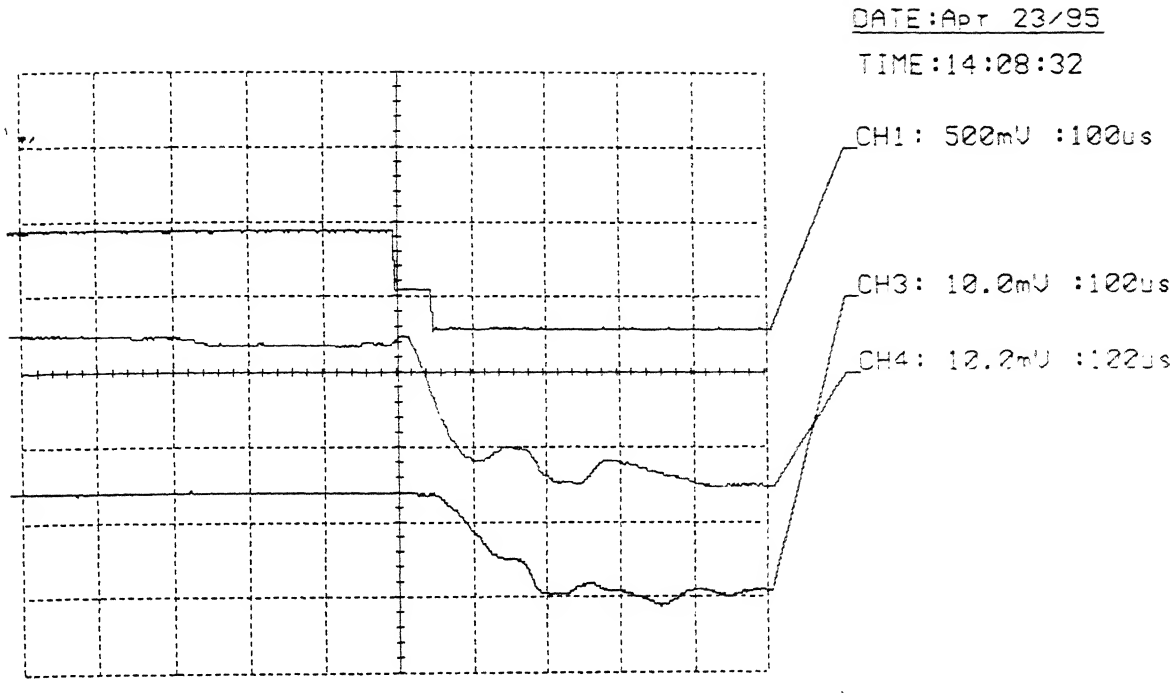

Fig. 4.3a Oscilloscope record for Expt. # 3

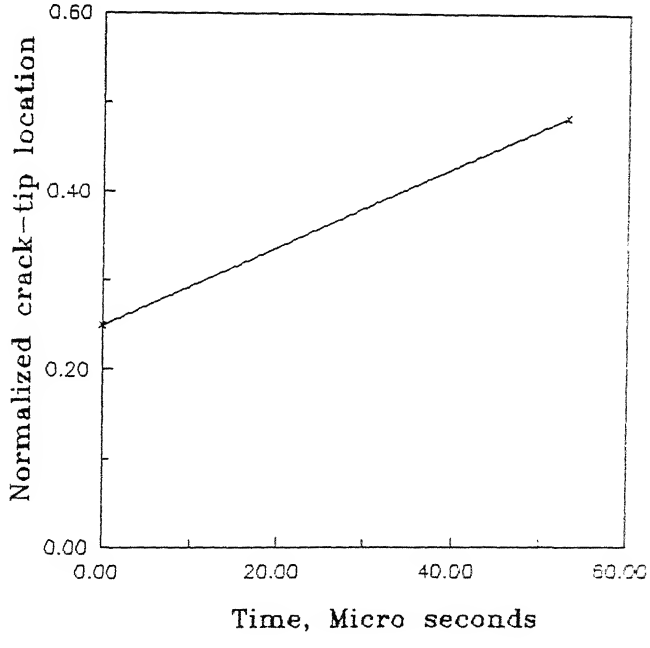

Fig. 4.3b Crack tip location as a function of time for Expt. # 3

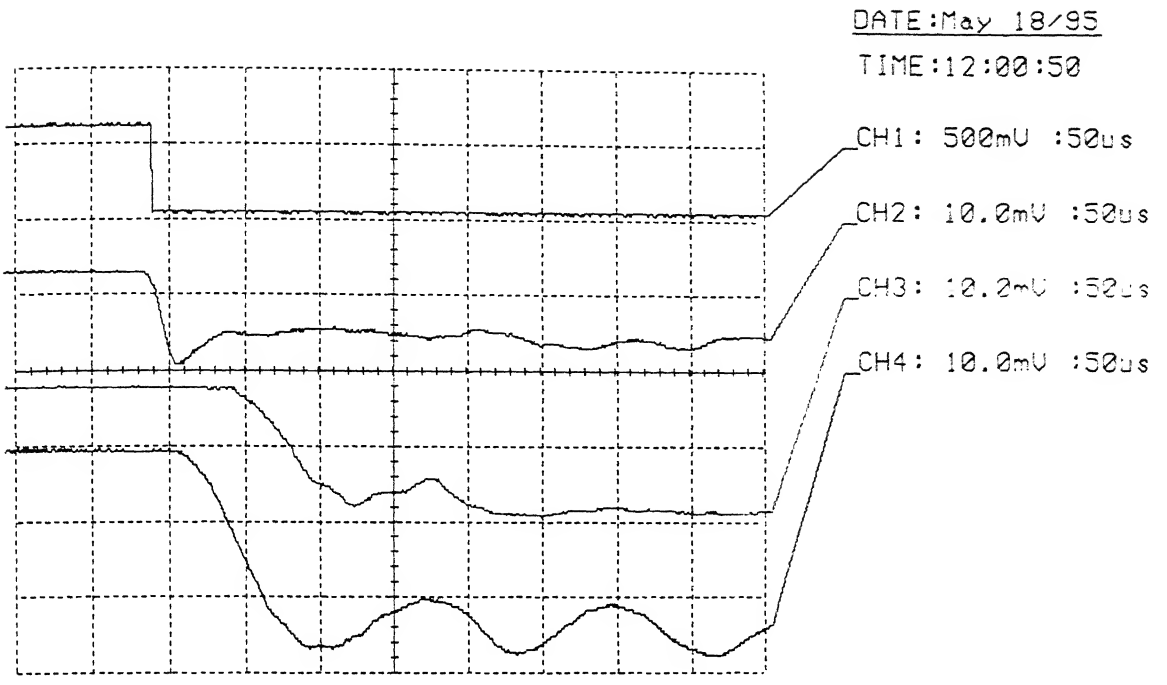

Fig. 4.4a Oscilloscope record for Expt. # 4

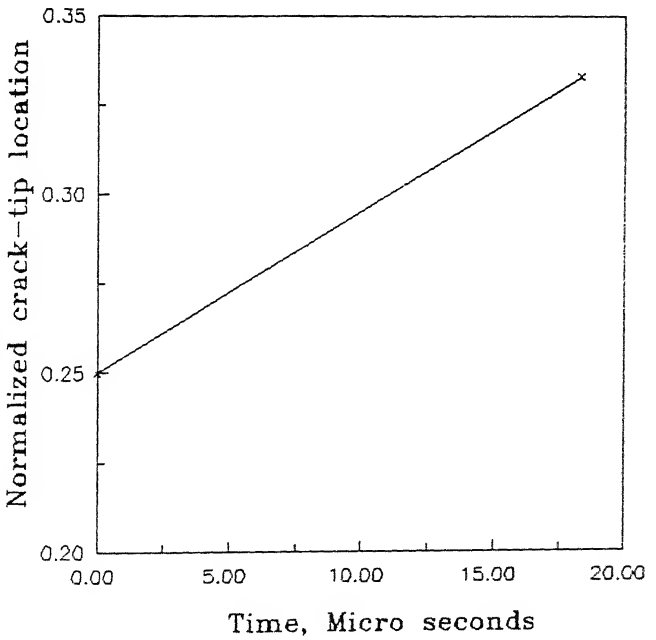

Fig. 4.4b Crack tip location as a function of time for Expt. # 4

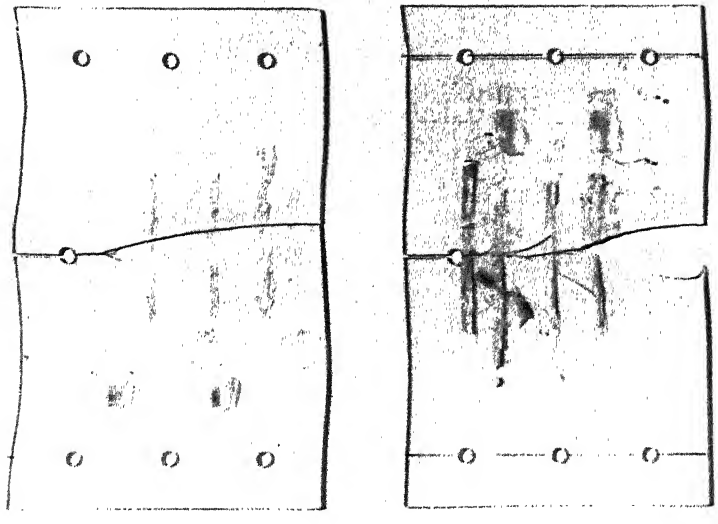

Fig. 4.5a : Photograph of the fractured specimen in Expt. # 3

Fig. 4.5b : Photograph of the fractured specimen in Expt. # 4

by manipulating the edge displacement till the recorded strain is obtained. This gives the displacement field in the static case. In the second stage, the above static displacement field is imposed as the initial condition in the dynamic analysis. Using the crack propagation of history and the dynamic FEM, the value of fracture toughness (J_1) is obtained as a function of normalized crack-tip position as explained in Sec. 2.9. For simplicity, The crack is assumed to have infinite acceleration.

The value of the normalized $\hat{J}_1$ ($\hat{J}_1/\hat{J}_{static}$) is plotted against the normalized crack-tip position in the Fig. 4.6 for Experiment No. 1. It is may be noted that the value of fracture toughness reduces to approximately one-half of its maximum value (at initiation) over a distance of about 3 mm before it starts raising. It may be due to the fact that, during this travel of 3 mm, most of the energy available is spent in accelerating the crack. However, since the total energy available is constant, the value of fracture toughness reduces. The value of fracture toughness starts increasing, as soon as the crack attains the constant velocity.

The variation of fracture toughness and crack-tip location with time for the experiments 2, 3 and 4 are plotted in Figs. 4.7 through 4.9. The value of the fracture toughness at branching ($\hat{J}_{1b}$) for the experiments 3 and 4 are tabulated in Table. 4.2. A high value of the $\hat{J}_{1b}$ in the experiment no. 4 may be due to the fact that in this case the crack travelled double the distance as compared to the experiment no. 3 before it branches and moreover it has taken a high load.

4.3 DISCUSSIONS

The fractured surface of the specimen for a typical experiment is shown in Fig. 4.10. The figure reveals that a smooth *mirror* finish surface extends upto a distance of about 3 mm from the initial crack-tip position. The value of stress intensity factor in similar mirror finish zone is observed to be less by Ravi-chander and Knauss (1984b). The surface roughness after this mirror finish zone increases along the crack path. Since the crack velocity is

observed to be constant from the experimental results along the crack path the crack surface roughness can be expected to be a direct consequence of the increasing fracture toughness. The value of fracture toughness increases due to the decrease in the strain energy of the specimen in fixed-grip condition.

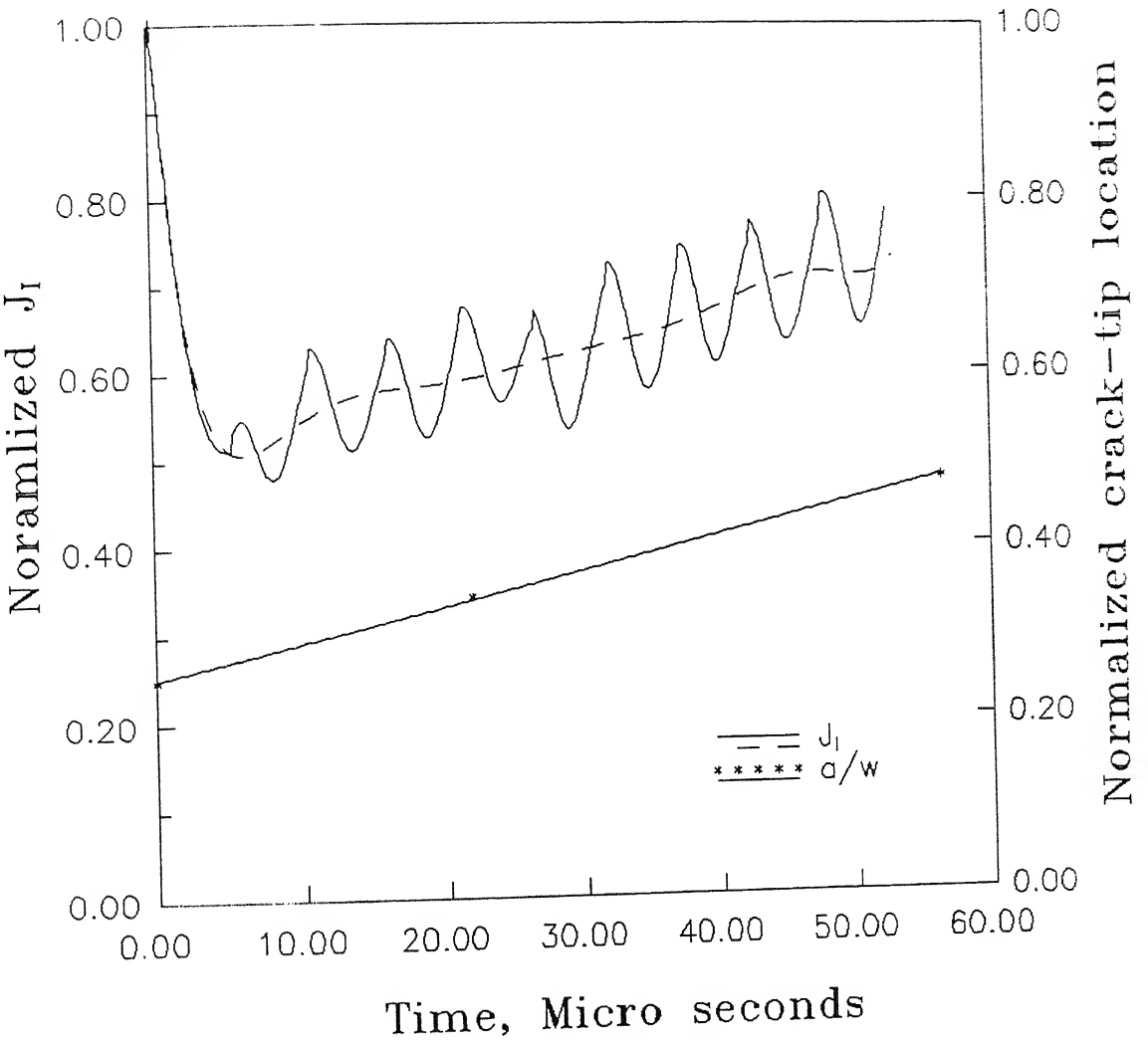

Fig. 4.6 $\hat{J}_1$ and crack-tip location as a function of time for Expt. # 1

$$\hat{J}_{static} = 7027 \text{ N/m}$$

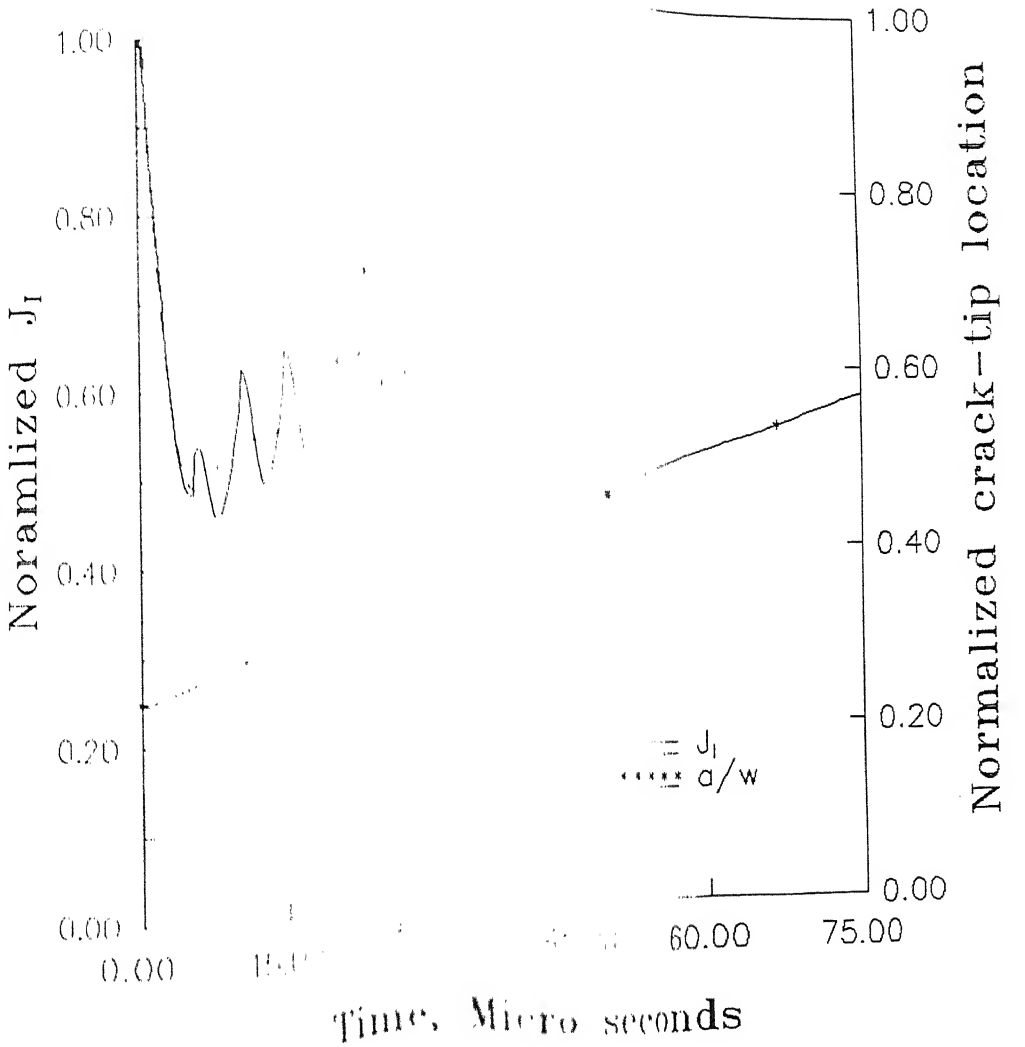

Fig. 4.7 J_I and crack tip location as a function of time for Expt. # 2

$J_{Q(ave.)}$ = 914.6 N/m

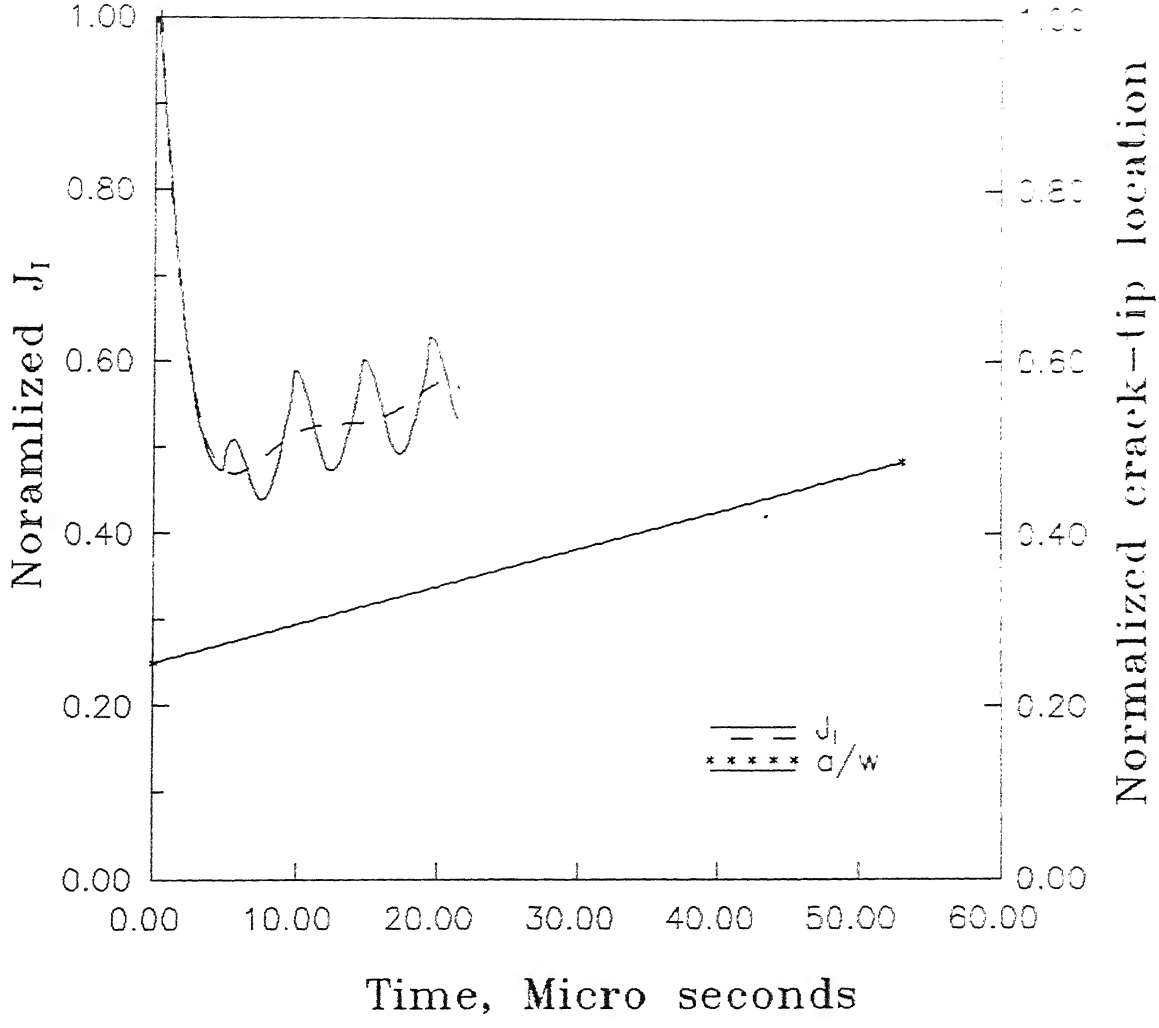

Fig. 4.8 $\hat{J}_1$ and crack-tip location as a function of time for expt. # 3

$\hat{J}_{static}$ = 10120 N/m

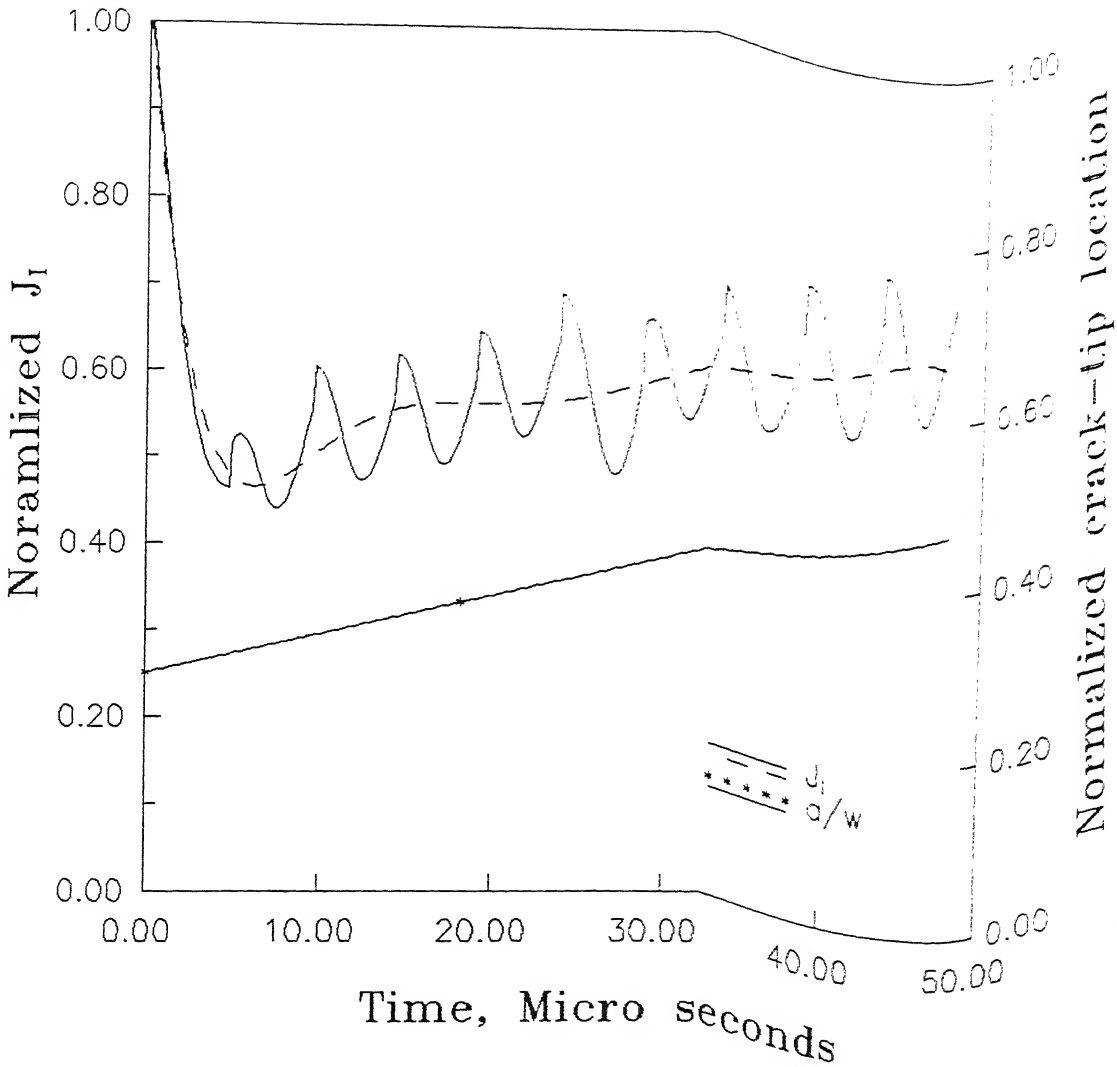

Fig. 4.9 $\hat{J}_1$ and crack-tip location as a function of time for expt. # 4

$$\hat{J}_{static} = 13774 \text{ N/m}$$

Fig. 4.10 Photograph of the fractured surface (50x)

Expt. #	Crack Velocity m/s	Pre-Strain μm/m		Remarks
		Gauge-1	Gauge-2	
1	512.29	4320	3200	No branching
2	552.24	---	3600	No branching
3	566.03	4707	4095	Branching at 26° after 12 mm from the crack-tip
4	578.70	5015	4596	Branching at 32° after 26.5 mm from the crack-tip

Table 4.1 Experimental observations and results

Expt.#	velocity	J_{1b} N/m
3	566.03	5570
4	576.70	9961

Table 4.2 Variation of J_{1b} with velocity

CHAPTER 5

CONCLUSIONS AND SCOPE FOR FURTHER WORK

Based in the hybrid experimental-numerical technique to measure the initiation and propagation fracture toughnesses for crack branching in PMMA, the following conclusions can be drawn.

a. The results indicate that the branching angle depends on the magnitude of the far field stress.

b. The instantaneous fracture toughness during propagation showed an increasing trend as the crack propagated in the model for all experiments.

c. The instantaneous fracture toughness reduced to about one-half of its value over a small distance at initiation before it starts raising. It may be due the fact that, during this time the kinetic energy starts building up.

d. The present analysis using limited number of experiments indicates a wide variation of fracture toughness at branching J_{1b} with velocity.

5.2 SCOPE FOR FUTURE WORK

1. The present method of analysis can be extended to study the variation of fracture

toughness as a function of the crack-tip location after branching.

A criterion for crack branching can be developed by performing more number of experiments and by using more sophisticated instrumentation such as high speed recording camera to record the crack-tip location as a function of time.

The experimental technique needs improvement to draw reliable conclusions on the material behavior in branching.

REFERENCES

Achenbach, G. D. (1974), Elasto-dynamic stress intensity factor for a bifurcating crack. *Prospects of fracture mechanics*, pp. 319-336.

Agarwal, B.D and Broutman, L.J (1990), Analysis and performance of fiber composites, 2nd edition, John-Wiley, New York.

Atluri, S. N. (1982), Path-independent integrals in finite elasticity and inelasticity, with body forces, inertia, and arbitrary crack face conditions. *Engg. Fracture Mech. 16*, pp. 341-364.

Atluri, S. N. and Nishioka, T. (1984), Hybrid method of analysis, *unification of finite element methods*, Ed. Kardestuncer, H., (north Holland, Amsterdam), pp. 65-96.

Bathe, K. J. (1982), Finite element procedures in engineering analysis., Printice-Hall Inc..

Burgers, P. and Dempsey, J. P. (1982), *Jl. of Applied Mechanics 49*, pp. 366-370.

Clark, A. B. J. and Irwin, G. R. (1966), *Experimental Mechanics 6*, pp. 321-330.

Dally, J. W., Fourney, W.L. and Irwin, G. R., (1985), On the uniqueness of the stress intensity factor - crack velocity relationship, *Int. Jl. Frac. 27*, pp. 159-168.

Eshleby, J. D (1970), in Inelastic behavior of solids, Ed. Kenninen, M. F. et al., Mc-Graw Hill, Newyork,

Felippa, C. A. (1974), Solution of linear equations with sky line-stored symmetric matrix. *J.C.A.S5*, pp. 13-29.

Field, J. (1971), Brittle fracture: its study and application. *Jl. of contemp. Phys. 12*, pp. 1-31.

Finkel, V. M. (1963), *Physics of metals and metallurgy 15*, 754-764.

Freund, L. B. (1972), Energy flux into the tip of an extending crack in an elastic solid, *Journal of Elasticity 2*, pp. 341-349.

Griffith, A. A. (1921), The phenomena of rupture and flow in solids, *Phil. Trans. Royal. Soc.*, London, A221, pp.163-197.

Griffith, A. A. (1924), The theory of rupture, *Proc. Ist Int. Congress Appl. Mech.*, pp. 55-63, Biezeno, Burgers Ed. Waltman (1925).

artzman, H and Hutchinson (1972), J.R Non-linear dynamics of the solids by finite ement method, *Computers and Structures 2*, pp. 44-77.

win, G. R. et al. (1979), On the determination of c-K relationship for birefringent olymers, *Experimental Mechanics 19*, pp. 121-128.

ileel, K. M, Finite element modelling of elastic wave interactions with cracks in composite aterials, *M.Tech thesis*, Indian Institute of Technology, Kanpur.

althoff, J. F. (1971), On the characteristic angle of crack branching in brittle materials, *Int. . Fracture Mech. 7*, pp. 478-480.

althoff, J. F. et al. (1977), Dynamic stress intensity factors for arresting cracks in DCB ecimens, *Fast fracture and crack arrest*, ASTM(STP) 627, pp. 161-176.

ishomoto, K.et al. (1980), On path independent integral J, *Engg. Fracture Mech. 12*, pp. 41-850.

obayashi, A. S. et al. (1974), Crack branching in Homolite-100 sheets. *Engg. frac. Mech.* , pp. 81-92.

obayashi, A. S et al. (1978), A numerical dynamic fracture analysis of three wedge loaded CB specimens, *Numerical Methods in Fracture Mechanics*, Eds. A.R.Luxmoore and .J.Owen (Univ. College, Swansea), pp. 673-684.

obayashi, T and Dally, J. W. (1977), The relation between crack velocity and stress ntensity factor in birefringent polymers, in *Fast fracture and crack arrest*, Hahn, G. T. and enninen, M. F, Eds., ASTM(STP) 627, pp. 257-273.

obayashi, A. S. and Mall, S. (1978), Dynamic fracture toughness of Homolite-100, *Experimental Mechanics 18*, pp. 11-18.

obayashi, A. S. (1983), Hybrid experimental-numerical stress analysis, *Experimental Mechanics 23*, pp. 338-347.

awn, B. R. and Wilshaw, T. R. (1975), Fracture in Brittle Solids, Cambridge University ress.

Malluck, J. F. and King, W. W (1978), Fast fracture simulated by finite-element analysis which accounts for crack-tip energy, *Numerical Methods in Fracture Mechanics*, Eds. A.R.Luxmoore and D.J.Owen (Univ. College, Swansea), pp. 648-659.

'. *ASCE 85*, pp. 67-94.

,hioka, T and Atluri, S. N. (1986), Computational methods in dynamic fracture, mputational methods in the mechanics of fracture, Edited by Atluri, S. N., pp. 336-383.

mulu, M and Kobayishi, A. S. (1984), Criteria for dynamic crack curving and Branching. *vances in Fracture Research 5*, Sixth Int. Conf. Fracture, New Delhi, India.

vi-chander, K. and Knauss, W. G. (1984a), An experimental investigation into dynamic cture: I. Crack initiation and arrest, *Int. Jl. of Fracture 25*, pp. 247-262.

vi-chander, K. and Knauss, W. G. (1984b), An experimental investigation into dynamic cture: II Microstructural aspects, *Int. Jl. of Fracture 26*, pp. 65-80.

vi-chander, K. and Knauss, W. G. (1984c), An experimental investigation into dynamic icture: III. On steady state crack propagation and branching, *Int. Jl. of Fracture 26*, pp. 1-154.

ıvi-chander, K. and Knauss, W. G. (1984d), An experimental investigation into dynamic icture: IV. On the interaction of stress waves with propagating cracks, *Int. Jl. of Fracture* , pp. 189-200.

ıy, A.K, 1994, Experimental investigation into dynamic interlaminar crack propagation in CB specimen, *M.Tech thesis*, Indian Institute of Technology, Kanpur.

ice, J. R. (1968), A path-independent integral and the approximate analysis of strain ıncentration by notches and cracks. *Jl. App.*
ech., pp. 379-386.

ydholm, G et al. (1978), Numerical investigations of rapid crack propagation, *Numerical 'ethods in Fracture Mechanics*, Eds. A.R.Luxmoore and D.J.Owen (Univ. College, Swansea),). 660-672.

chardin, H. (1959), in Fracture, Ed. Averbach et al., John Wiley.

hukla, A and Anand, S (1986), Dynamic crack propagation and branching under biaxial ıading, *Fracture Mechanics: Seventeenth Volume, ASTM STP 905*, J.H.Underwood, R.chait, *I*.smith, D.P.Withem, W.A Andrews and J.C. Newmann, Eds., American Society of Testing laterials, Philadelphia, pp.(697-714).

ih, G,C (1977), Introductory chapter in elasto-dynamic problems, Mechanics of fracture IV.

hukla, A., Nigam, H. and Zervas (1990), H, Effect of stress field parameters on dynamic

rack branching, *Engg. Frac. Mech 36, 3,* pp. 429-438.

)hukla, A and Anand, S (1986), Dynamic crack propagation and branching under biaxial oading, *Fracture Mechanics: Seventeenth Volume, ASTM STP 905*, J.H.Underwood, R.chait, N.smith, D.P.Withem, W.A Andrews and J.C. Newmann, Eds., American Society of Testing Materials, Philadelphia, pp.(697-714).

Theocaris, T and Georgidis, H. G. (1985), Bifurcation prediction for moving cracks by T-criterion. *Int. Jl. Fracture 29,* 181-190.

Yoffe, E. (1951), The moving Griffith crack, *Phil. Mag. Ser. 7, 42,* pp. 739-750.

APPENDIX-A

SHAPE FUNCTIONS AND MATERIAL PROPERTY MATRICES

iis appendix gives the shape functions and the derivatives of the isoparametric four noded ement and the material property matrices.

iape functions for the isoparametric four noded element :

i natural coordinates each finite element is a square centered at origin having vertices at 1,-1), (1,-1), (1,1), (-1,1).

$$N_j(\xi,\eta) = \frac{1}{4}(1+\xi\xi_j)(1+\eta\eta_j) \qquad for\ j = 1,2,3,4 \qquad (A.1)$$

'he derivatives of the shape functions are given by :

$$B = \begin{bmatrix} -\frac{(1-\xi)}{4} & 0 & \frac{(1+\xi)}{4} & 0 & \frac{(1+\xi)}{4} & 0 & -\frac{(1-\xi)}{4} & 0 \\ 0 & -\frac{(1-\eta)}{4} & 0 & -\frac{(1-\eta)}{4} & 0 & \frac{(1+\eta)}{4} & 0 & \frac{(1+\eta)}{4} \\ -\frac{(1-\eta)}{4} & -\frac{(1-\xi)}{4} & -\frac{(1-\eta)}{4} & \frac{(1+\xi)}{4} & \frac{(1+\eta)}{4} & \frac{(1+\xi)}{4} & \frac{(1+\eta)}{4} & -\frac{(1-\xi)}{4} \end{bmatrix} \qquad (A.2)$$

Material property matrices :

For isotropic materials in plane stress :

$$D = \frac{E}{(1-\nu^2)} \begin{bmatrix} 1 & \nu & 0 \\ \nu & 1 & 0 \\ 0 & 0 & \frac{1-\nu}{2} \end{bmatrix} \qquad (A.3)$$

For isotropic materials in plane strain :

$$D = \frac{E(1-\nu)}{(1+\nu)(1-2\nu)} \begin{bmatrix} 1 & \frac{\nu}{(1-\nu)} & 0 \\ \frac{\nu}{(1-\nu)} & 1 & 0 \\ 0 & 0 & \frac{(1-2\nu)}{2(1-\nu)} \end{bmatrix} \qquad (A.4)$$

For orthotropic materials [Agarwal & Broutman, 1990] :

$$D = \begin{bmatrix} \bar{Q}_{11} & \bar{Q}_{12} & \bar{Q}_{16} \\ \bar{Q}_{21} & \bar{Q}_{22} & \bar{Q}_{26} \\ \bar{Q}_{31} & \bar{Q}_{23} & \bar{Q}_{66} \end{bmatrix} \qquad (A.5)$$

where $[\bar{Q}]$ is the off-axis lamina stiffness.